Karlsruher Institut für Technologie

Horizon2020
European Union Funding
for Research & Innovation

electronic hydrodynamics

Boris Narozhny

Institute for Theoretical Condensed Matter Physics, KIT

DFG

FLAG-ERA

hydrodynamic approach

describes a wide variety of systems and phenomena: water flow, atmospheric phenomena, plasma, interstellar medium

- why not electrons in solids?

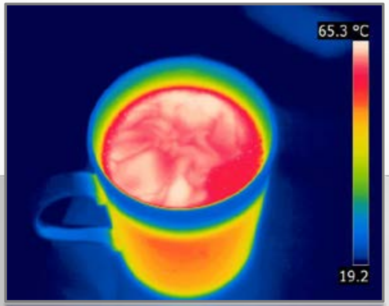

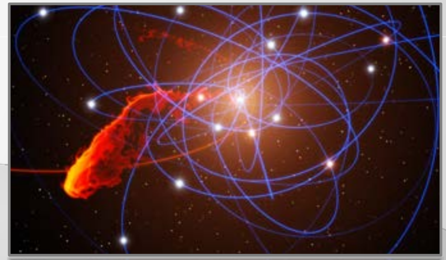

why is it so hard for electrons to behave collectively?

unlike fluid molecules, electrons in solids exist in the environment formed by a crystal lattice

impurity scattering

low-temperature transport is typically dominated by potential disorder responsible for residual resistivity

electron-phonon scattering

high-temperature transport is determined by scattering off lattice vibrations - phonons

intermediate temperatures

$$\tau_{ee} \ll \tau_{\rm dis}, \tau_{\rm ph} \qquad\qquad T_{\rm dis} \ll T \ll T_{\rm ph}$$

hydrodynamic behavior is established by electron-electron interaction which may dominate in an intermediate temperature window, that is not guaranteed to exist

four topics in condensed matter theory

kinetic equation

- quasiparticle approximation
- linear response theory
- macroscopic currents

electronic transport

- linear response
- macroscopic transport theory
- T and B dependence of R

graphene

- ultra-pure material
- unconventional hydrodynamics at charge neutrality

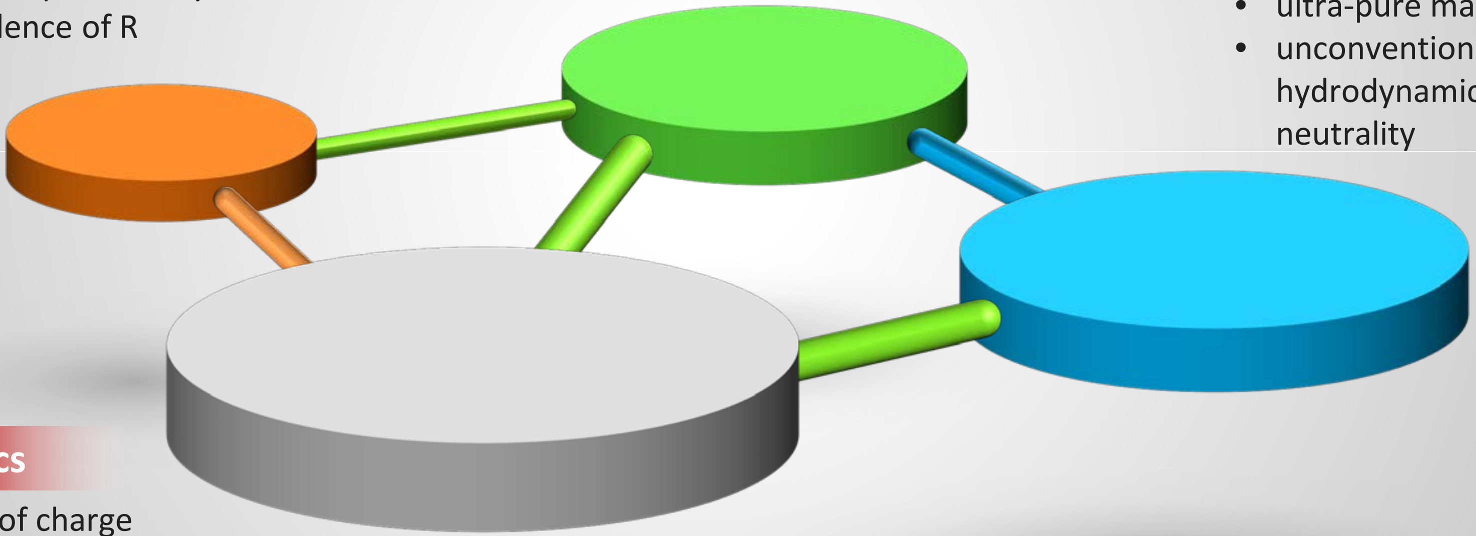

hydrodynamics

- collective flow of charge and energy
- viscous dissipation
- *“better than ballistic” conduction*

foreword: traditional approach to transport

predominantly “one-electron” approach to solids

standard linear response theory – bulk systems

phenomenological description of transport properties reflecting the observed linear relation between the driving bias and measured response

Ohm's Law

Ziman (1962)

electric and heat currents

$$\boldsymbol{J} = \sigma \boldsymbol{E} - \sigma\alpha \boldsymbol{\nabla} T$$

$$\boldsymbol{Q} = \sigma\alpha T \boldsymbol{E} - (\kappa + \sigma\alpha^2 T)\boldsymbol{\nabla} T$$

Drude formula

$$\sigma = \frac{e^2 n\tau}{m^*}$$

thermal conductivity

$$\kappa = \frac{\pi^2 T}{3e^2}\sigma$$

thermoelectric power

$$\alpha = \frac{\pi^2 T}{3e}\frac{1}{\sigma}\left.\frac{\partial\sigma}{\partial\epsilon}\right|_{\epsilon=E_F}$$

Hall coefficient

$$R_H = \frac{1}{nec}$$

Wiedemann-Franz Law

Ziman (1962)

Lorentz number

$$L = \frac{\kappa}{\sigma T} \quad \Rightarrow \quad L_0 = \frac{\pi^2}{3e^2}$$

copper

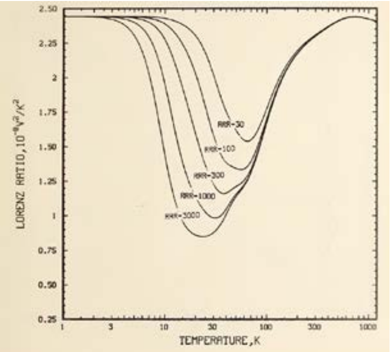

National Bureau of Standards (1984)

temperature dependence of resistivity: "conventional" metals

typical experiments measure resistivity as a function of temperature and magnetic field

copper (engineer's view)

Springer Handbook (2017)

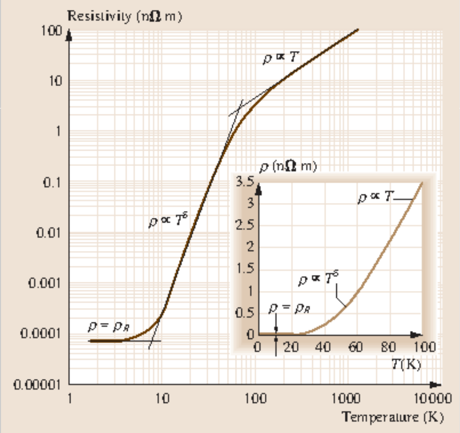

$E_F = 7\,\mathrm{eV}$

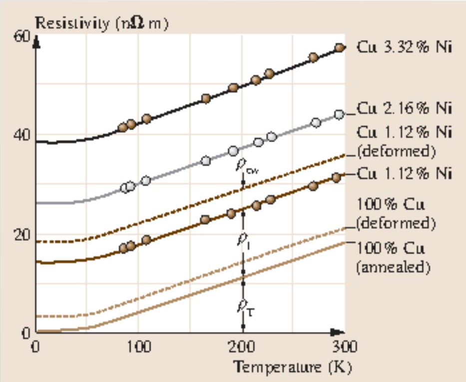

$\rho(T > T_D) \propto T$

$\rho(T < T_D) \propto T^5$

iron

Yousuf et.al. (1986)

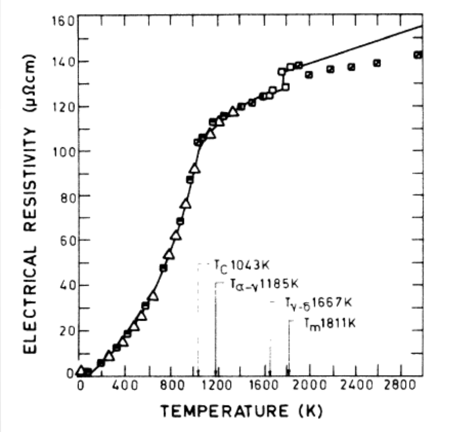

$E_F = 11\,\mathrm{eV}$

$\rho(T > T_c) \propto T$ $\rho(T < T_c) \propto T^2$

temperature dependence of electrical resistivity: “strange” metals

transport experiments yield linear in T resistivity in wide parameter intervals “unexpected” from the conventional viewpoint, (e.g., in contrast to the T^2 behavior)

linear resistivity in solids

Bruin et.al. (2013)

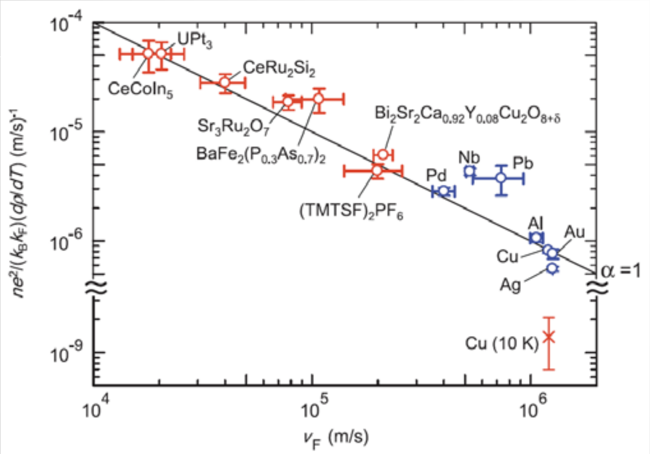

linear resistivity in $Bi_2Sr_2CuO_{6+\delta}$

Hartnoll and Mackenzie, RMP (2022)

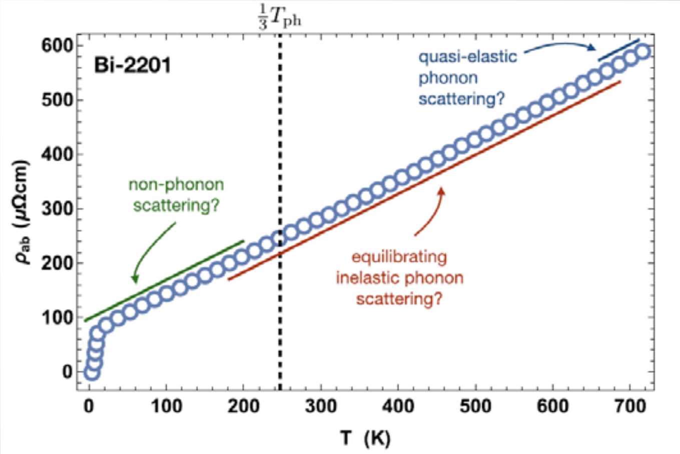

temperature dependence of resistivity: "conventional" metals

typical experiments measure resistivity as a function of temperature and magnetic field

T^2 behavior in non-magnetic metals

Poker, Klabunde (1982)

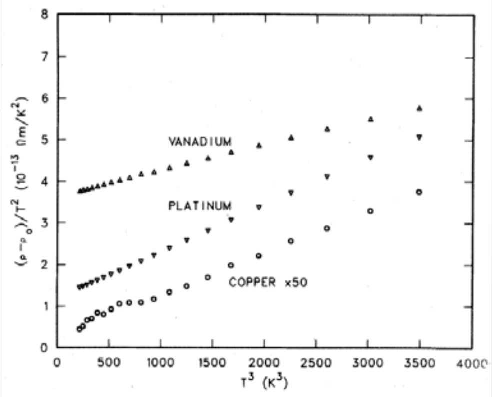

$$\rho(T < T_D) = \rho_0 + aT^2 + bT^3 + cT^5$$

data supports T^2 term in the range 6-12 K

data does not support T^2 term over the whole range 6 – 327 K

2D electron systems in heterostructures

Spivak et.al. RMP (2010)

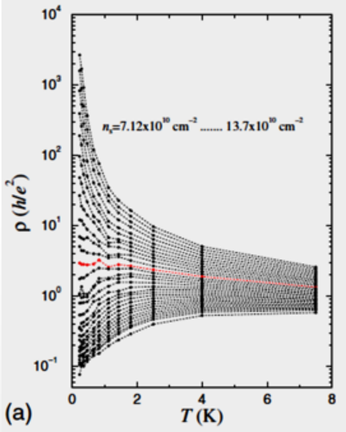

$$E_F = \frac{\pi n}{2m^*} \approx 0.58\,\mathrm{eV}$$

at

$$n = 10^{11}\,\mathrm{cm}^{-2}$$

$$T_F \approx 7\,\mathrm{K}$$

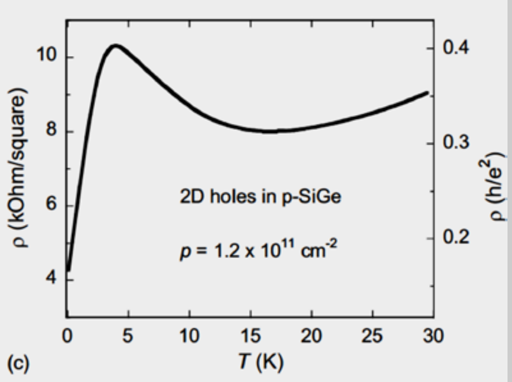

temperature dependence of resistivity: “conventional” theory

different powers □□ $T^{\square}$ can be obtained for different scattering processes, Fermi surface shapes, carrier densities, etc.

resistivity due to phonons

Ziman (1962)

electron-phonon scattering, low temperatures

$$\rho(T < T_D) \propto T^5$$

spherical Fermi surface, no Umklapps, phonons in equilibrium

electron-phonon scattering, high temperatures

$$\rho(T > T_D) \propto T$$

phonons in classical equipartition regime

electron-phonon scattering, small cylindrical Fermi surface

Kukkonen (1978)

$$\rho \propto T^2$$

mechanisms of T^2 dependence

Umklapp scattering

Landau, Pomeranchuk (1937)

two-band scattering

Baber (1937)

electron-magnon scattering

Mott (1964)

Coulomb drag

Pogrebinsky (1977)

resistance due to viscosity: Gurzhi effect

transition from Knudsen to Poiseuille flow in clean, narrow samples

resistance minimum

Gurzhi (1963)

$$\ell_{ee} \ll d$$

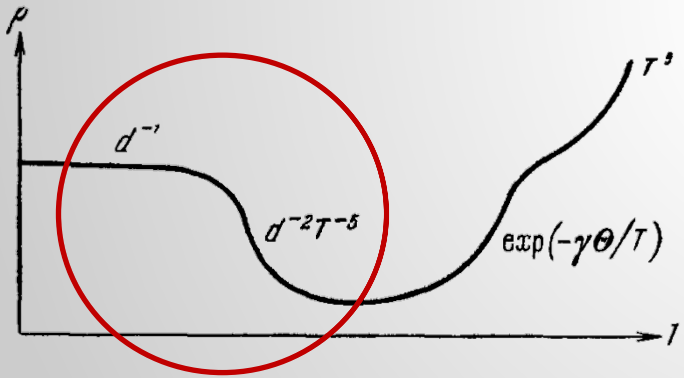

non-monotonic differential conductance

de Jong, Molenkamp (1995)

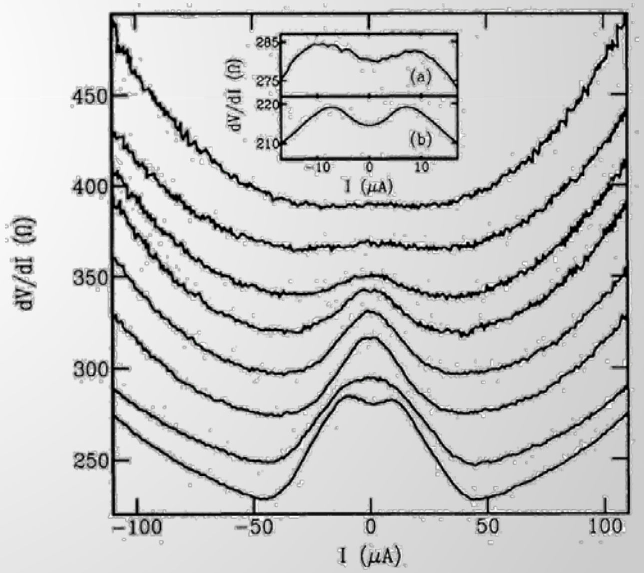

Knudsen vs Poiseuille flow

transition from Knudsen to Poiseuille flow in clean, narrow samples

Knudsen flow

Knudsen (1909)

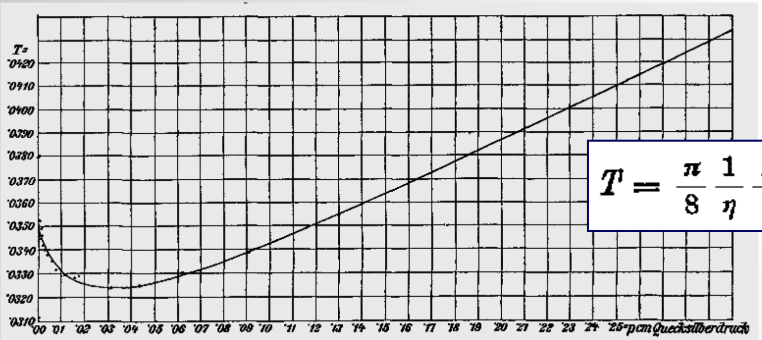

Fig. 4b. Kohlensäure. Die Röhre 4.

$$T = \frac{\pi}{8}\,\frac{1}{\eta}\,\frac{R^4}{L}\,p$$

high Knudsen number:
tube size same or smaller than mean-free path

independent molecular flow
minimum in gas-flow rate

Poiseuille flow

Poiseuille (1840)

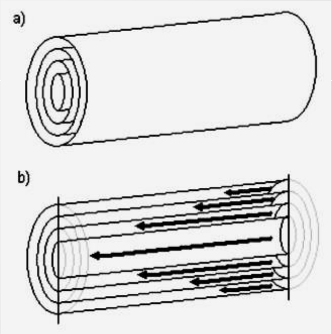

incompressible fluid

no-slip boundary condition

laminar flow

parabolic velocity profile

electronic hydrodynamics

lecture 1: experiment

nonlocal resistance

vorticity, ballistic motion, or edge charge accumulation?

nonlocal transport in graphene

initial attempt at detecting non-uniform current flows

degenerate regime: negative local resistance

Geim group (2016)

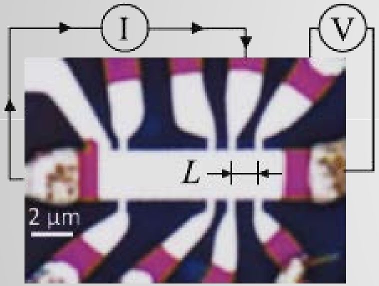

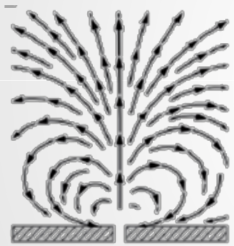

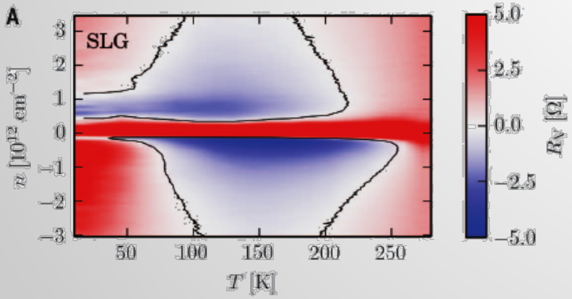

neutral graphene: giant nonlocality

Geim group (2011)

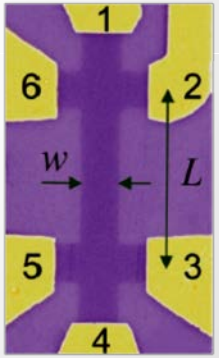

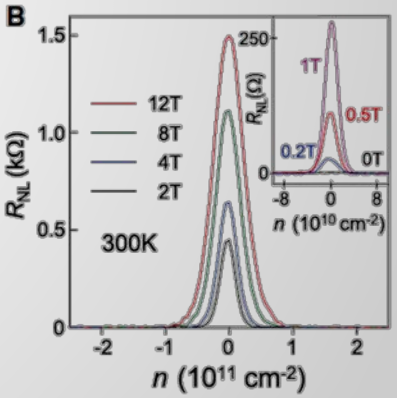

electron hydrodynamics beyond graphene

electron hydrodynamics can be observed in suitable materials

palladium cobaltate (PdCoO2)

Mackenzie group (2016)

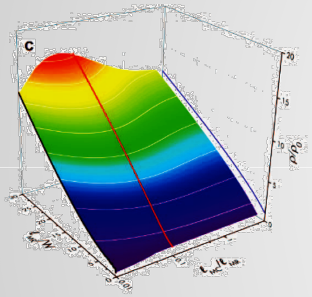

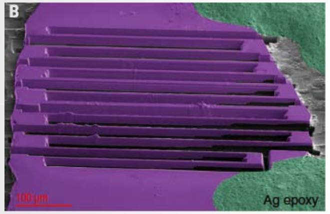

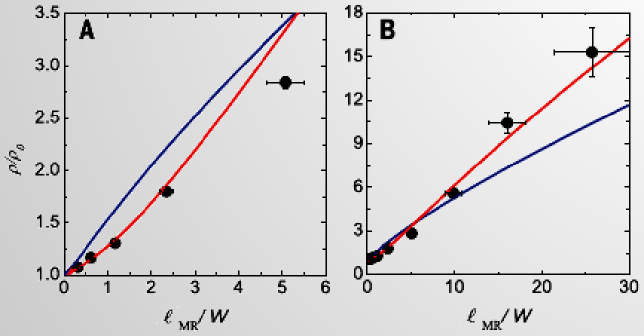

topological materials (WP2)

Felser group (2018)

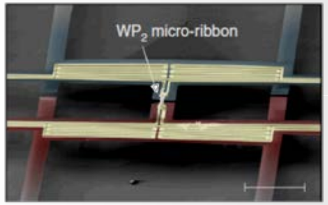

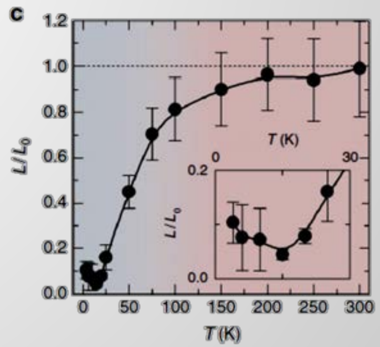

effect of viscosity on electron flow in doped graphene

results of nonlocal transport measurements can be interpreted with the help of a hydrodynamic approach; negative vicinity resistance can be attributed to vorticity of the electronic fluid.

Poiseuille flow

Torre, Tomadin, Geim, Polini (2015)

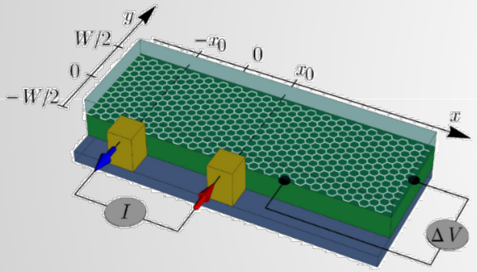

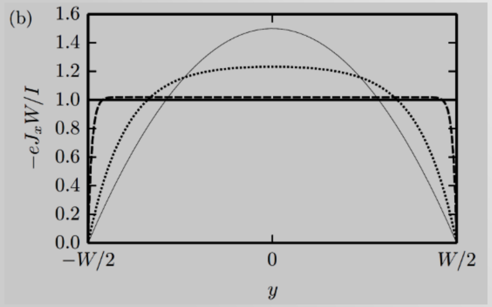

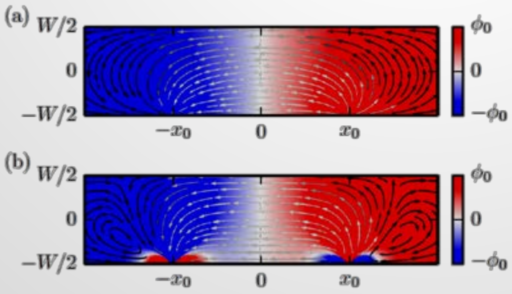

Ohmic vs viscous flow

Levitov, Falkovich (2016)

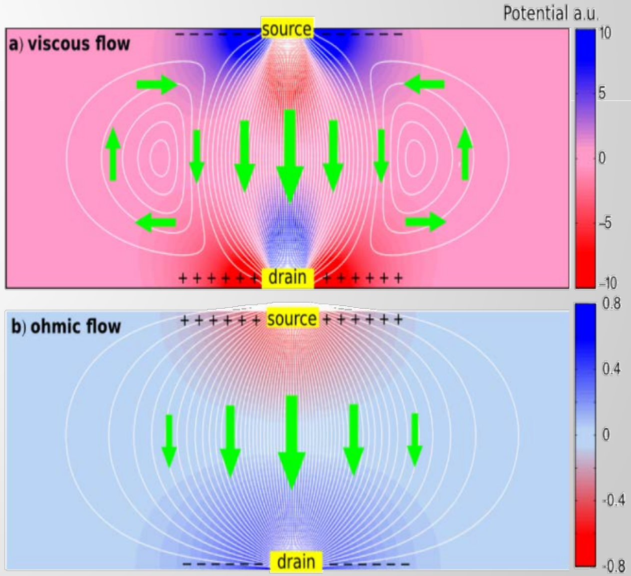

electron hydrodynamics vs ballistics

some observed phenomena can be explained not only by a hydrodynamic but also by a ballistic transport

fluidity onset in graphene

Geim group (2018)

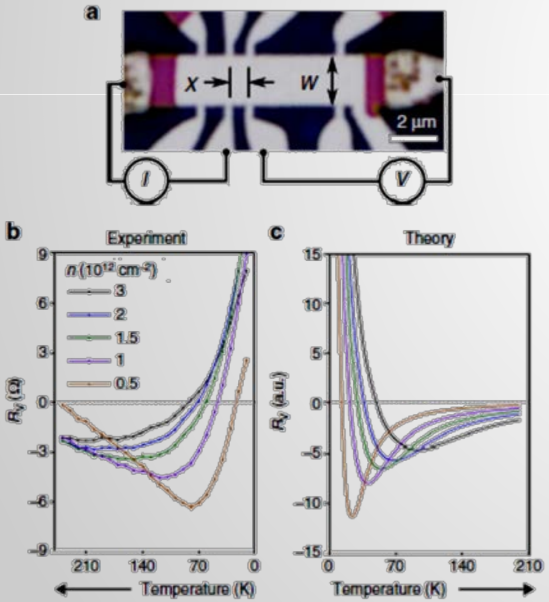

current density imaging

Weizmann group (2019)

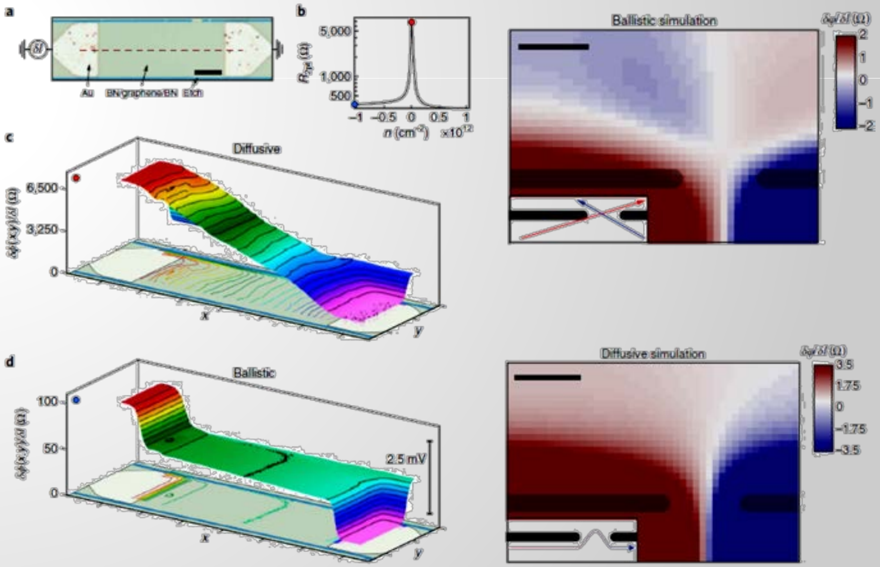

diffusive to ballistic crossover

in confined geometries, electron motion is governed by the ratio of the mean free path to the sample size

boundary conditions for distribution function

Beenakker, van Houten (1991)

slab geometry

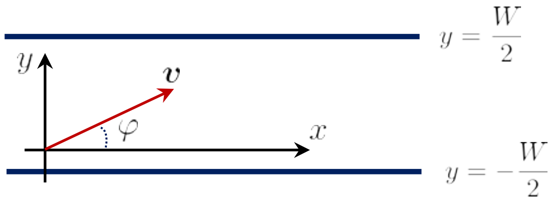

diffusive scattering at the boundary

$$f = f_0 + \delta f(y, \varphi)$$

$$\delta f\left(\frac{W}{2}; -\pi < \varphi < 0\right) = \frac{1}{2}\int_0^{\pi} d\varphi' \cos\varphi' \delta f\left(\frac{W}{2}; \varphi'\right)$$

outgoing *incoming*

current profile in the slab geometry

$$J_x \propto 4\int_0^1 dz\sqrt{1-z^2}\left[1 - e^{-\frac{1}{\ell z}}\cosh\frac{y}{\ell z}\right]$$

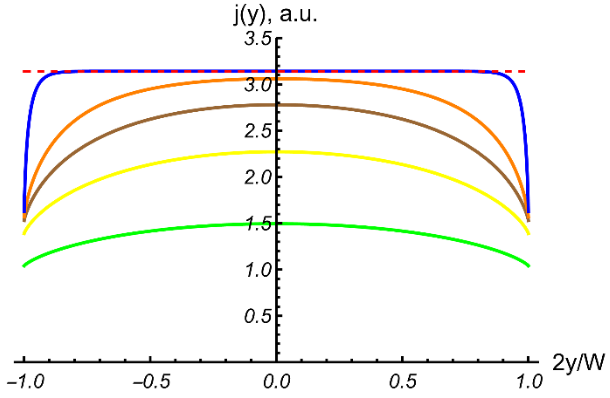

edge currents due to edge charge accumulation

classical edge physics may be masking more interesting bulk phenomena; Zeldov group (2020)

edge charge accumulation

band bending

electrostatic gating

charged impurities

Quantum Hall edge state

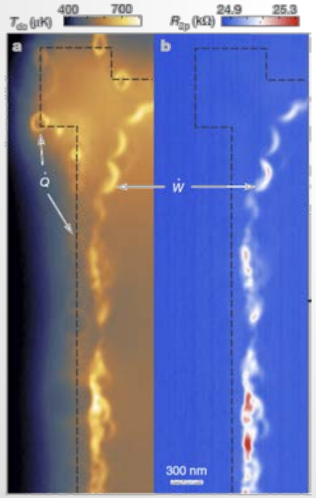

LDoS in G/hBN wire (DFT)

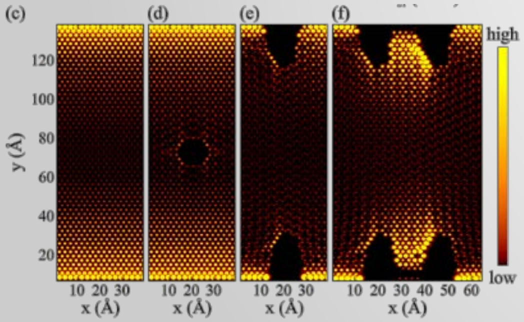

Marmolejo-Tejada et.al (2018)

Marguerite et.al (2019)

experimental observations

non-decaying non-topological edge current in magnetic field (leading to nonlocal transport)

local potential (scanning tip) is able to stop the edge current

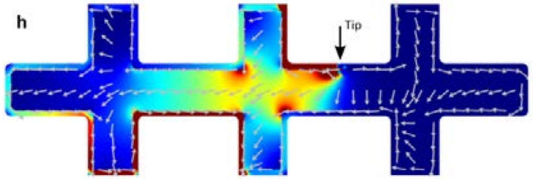

numerical solution of hydrodynamic equations

Danz, BN (2020)

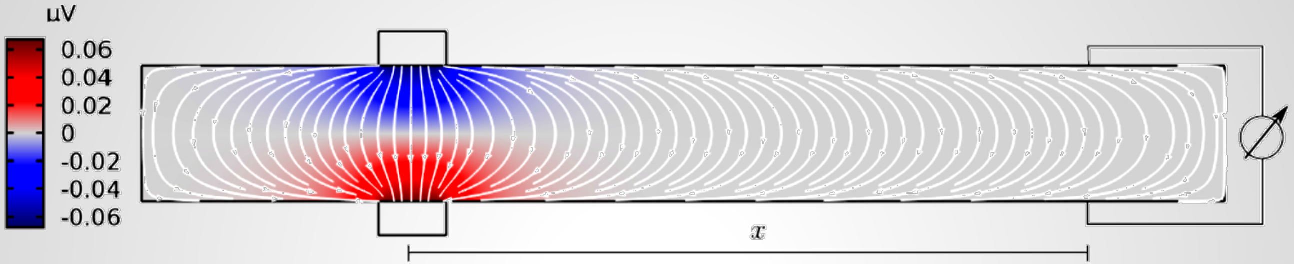

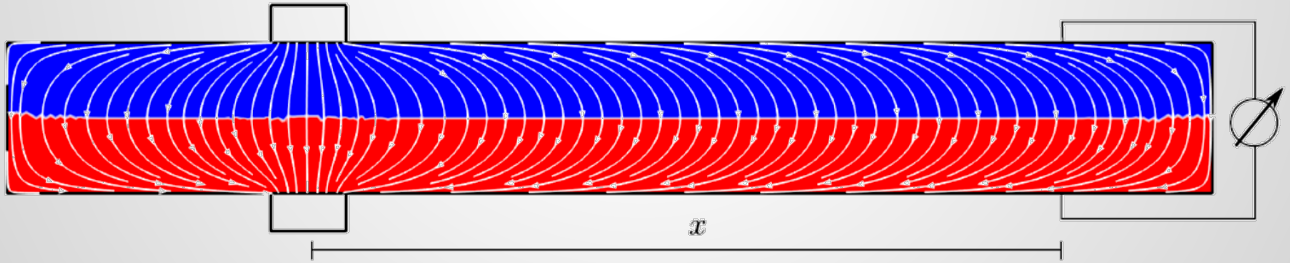

numerical solution of hydrodynamic equations

Danz, BN (2020)

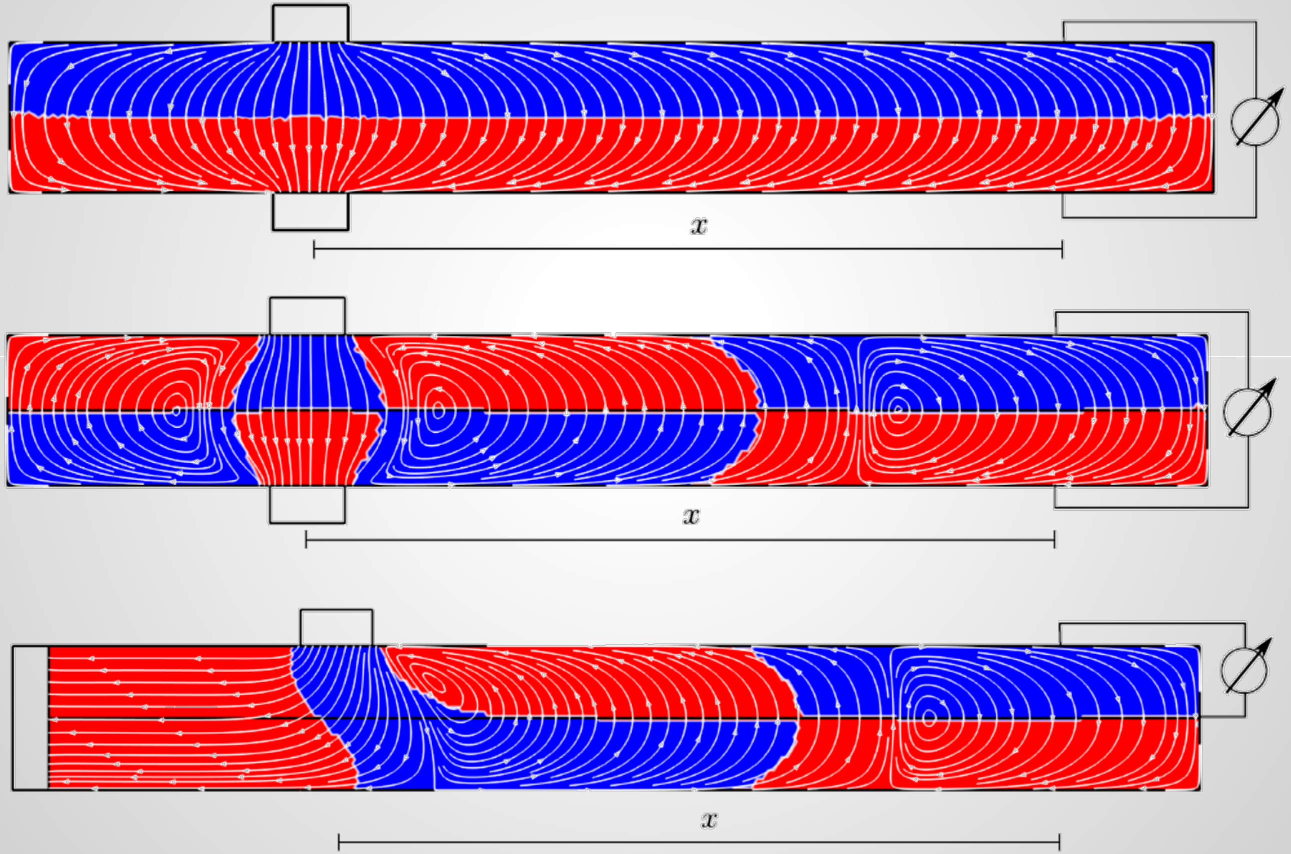

direct observation of vortices

vortices are the hallmark of viscous flows, however, in certain geometries they may appear also in the ballistic regime;
SOT temperature 4 K, electron temperature up to 18 K

laminar vs vortical flow

Zeldov group (2022)

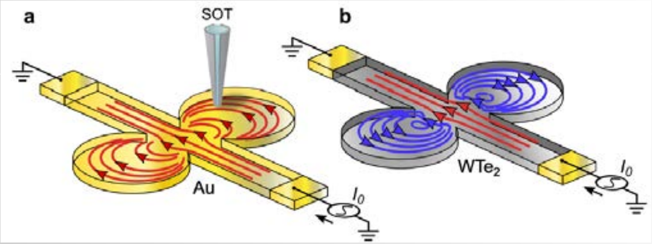

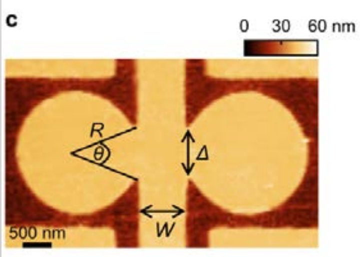

Ohmic vs viscous flow

Zeldov group (2022)

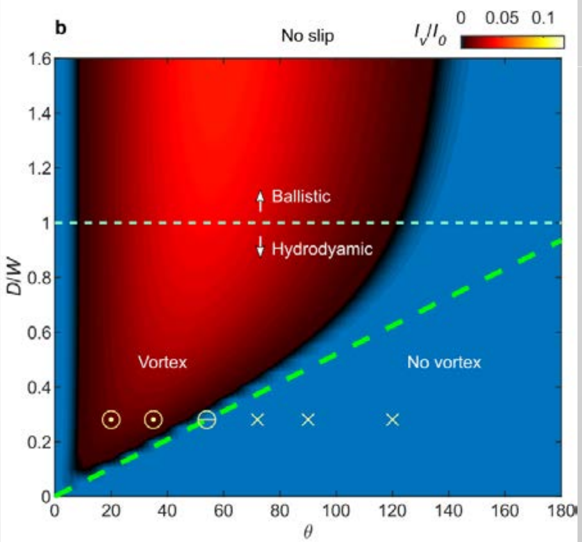

direct observation of vortices

vortices are the hallmark of viscous flows, however, in certain geometries they may appear also in the ballistic regime;
SOT temperature 4 K, electron temperature up to 18 K

Ohmic flow in Au films

Zeldov group (2022)

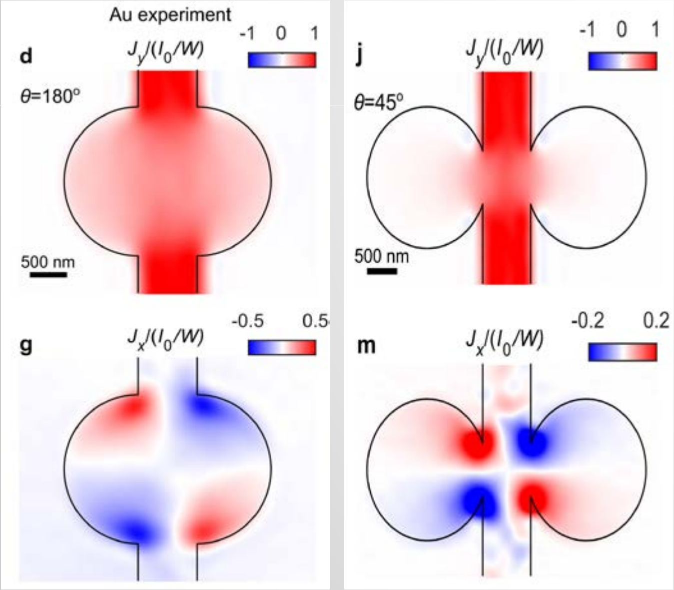

vortices in WTe_2

Zeldov group (2022)

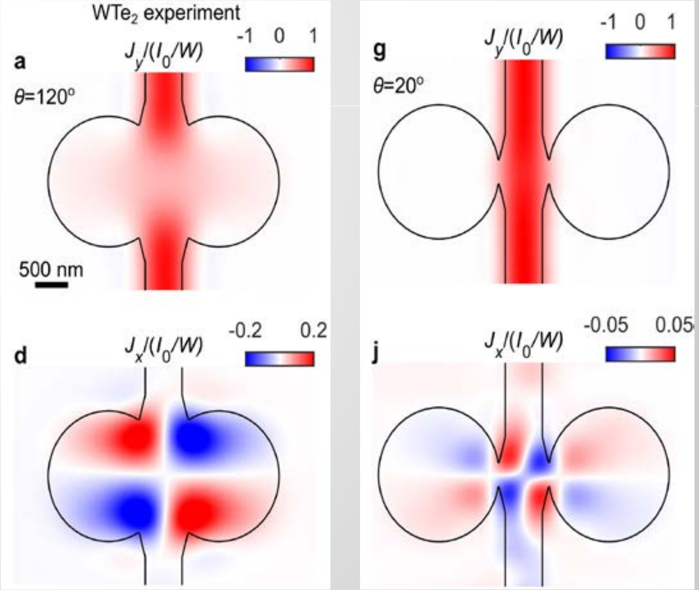

direct observation of vortices

double vortices are only expected in the hydrodynamic regime; SOT temperature 4 K, electron temperature up to 18 K

Ohmic flow in Au films

Zeldov group (2022)

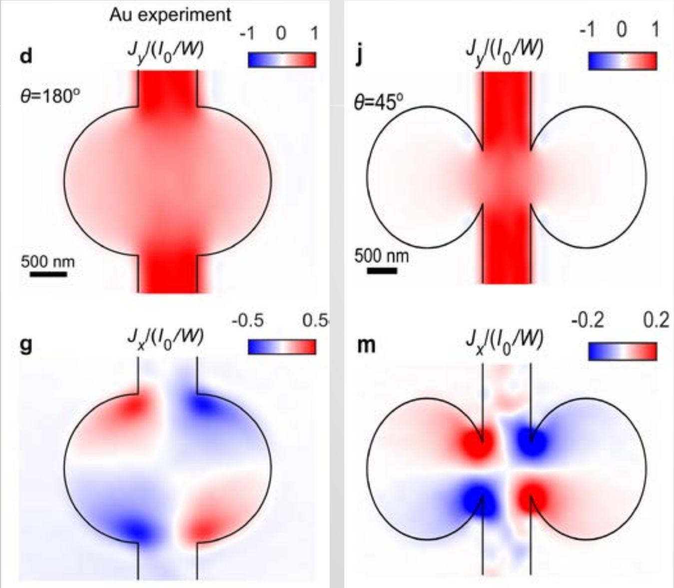

double vortex in WTe_2

Zeldov group (2022)

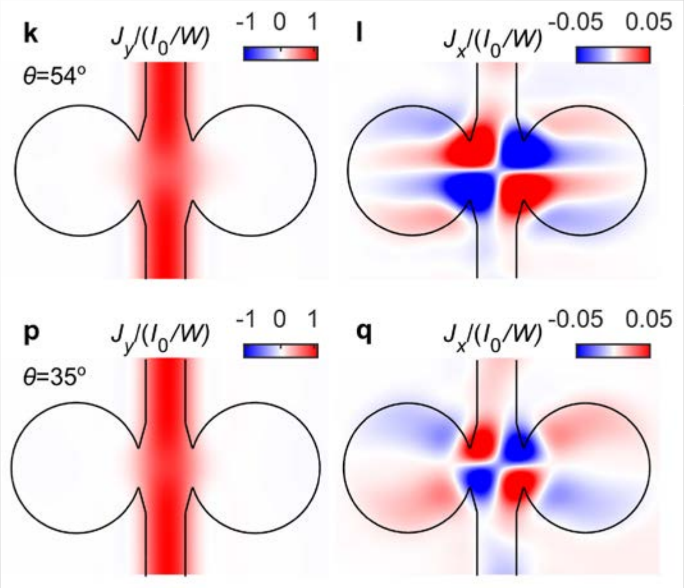

viscous flow of charge

superballistic transport, Poiseuille flow

simplest manifestation of viscosity – Poiseuille flow

Landau, Lifshitz, vols. 6, 10

Poiseuille flow in a tube

Poiseuille (1840)

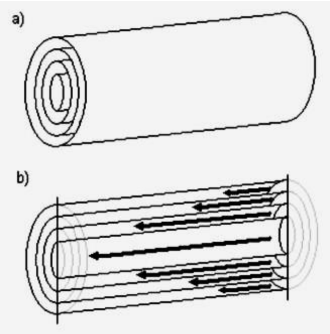

$$\nabla p = \eta \Delta \boldsymbol{v}$$

$$u_z = -\frac{\partial p}{\partial z}\frac{R^2 - r^2}{4\eta}$$

$$u_r = u_\theta = 0$$

$$I = \frac{\pi n R^4}{8\eta l}\delta p$$

incompressible fluid

no-slip boundary conditions

parabolic velocity profile

Poiseuille flow in the presence of obstacles

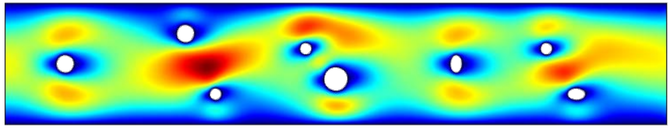

flows around obstacles avoiding scattering

flow rate exceeding independent molecular flow (Knudsen flow)

key to understand superballistic transport experiments in graphene

electronic flow around an obstacle

Gusev et.al. (2020)

Poiseuille flow in a Hall bar (*GaAs*)

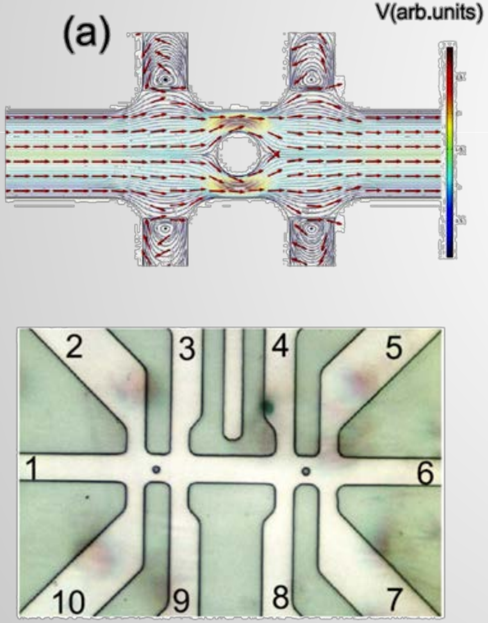

electron-electron relaxation rates

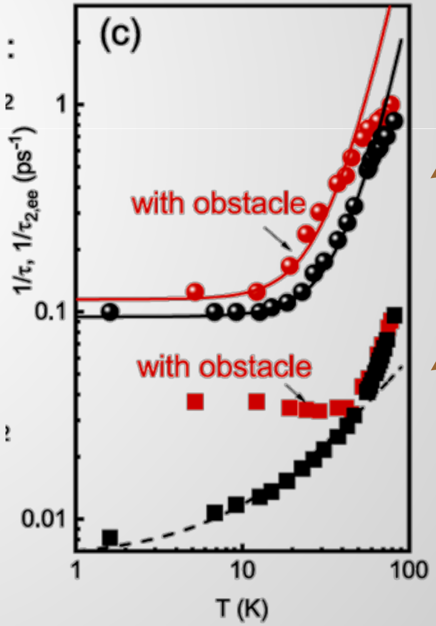

$\frac{1}{\tau_{ee}}$

$\frac{1}{\tau}$

superballistic transport

electrons can flow around obstacles similarly to a viscous fluid (instead of scattering)

experiment (flow through constrictions)

Geim group (2017)

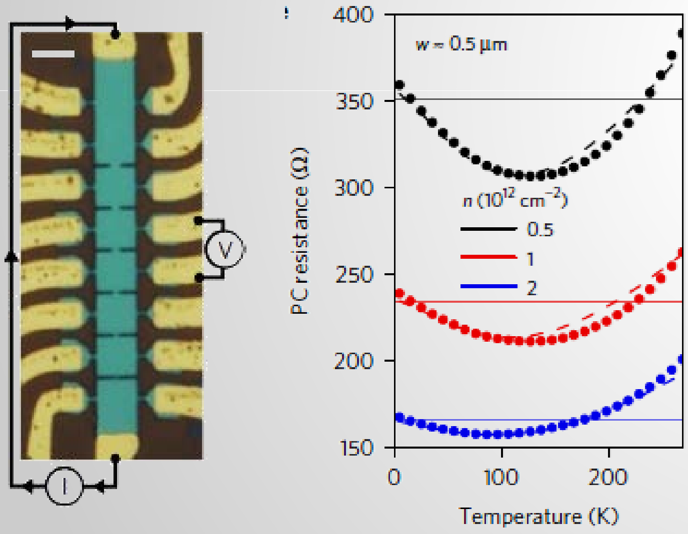

Stokes flow vs ballistic flow

Guo, Ilseven, Falkovich, Levitov (2017)

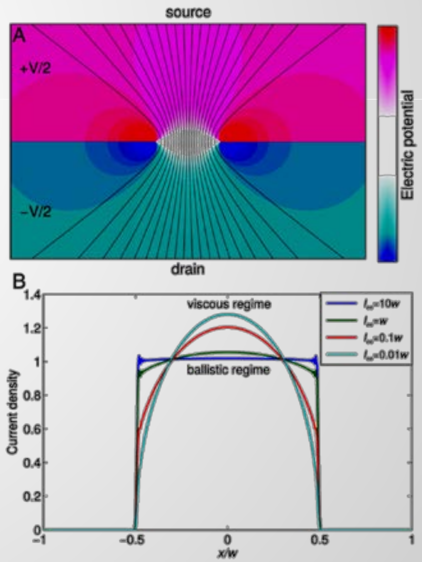

superballistic transport

imaging of the current profile highlighting the importance of boundary conditions

measured current profiles

Young group (2020)

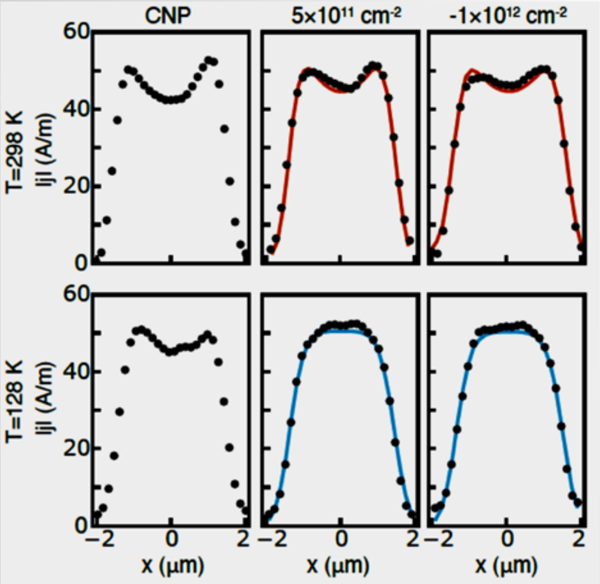

calculated current profiles

Pershoguba, Young, Glazman (2020)

$$[\eta\,\Delta - (ne)^2\rho\,]\,\boldsymbol{v}(\boldsymbol{r}) = ne\boldsymbol{\nabla}\phi(\boldsymbol{r})$$

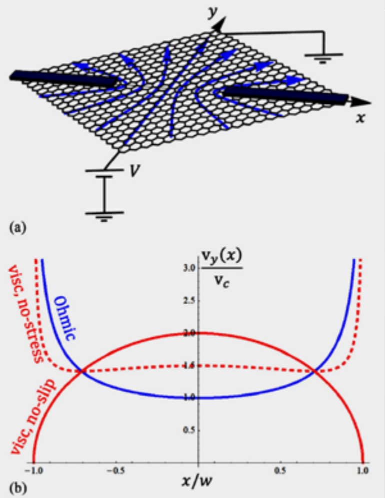

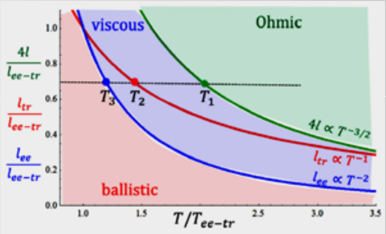

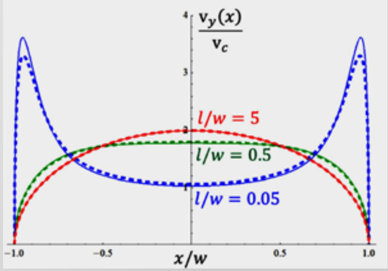

electronic flow in a narrow channel

local probes allow to determine local current density and uncover Poiseuille flows

scanning nanotube SET – doped graphene

Weizmann group (2019)

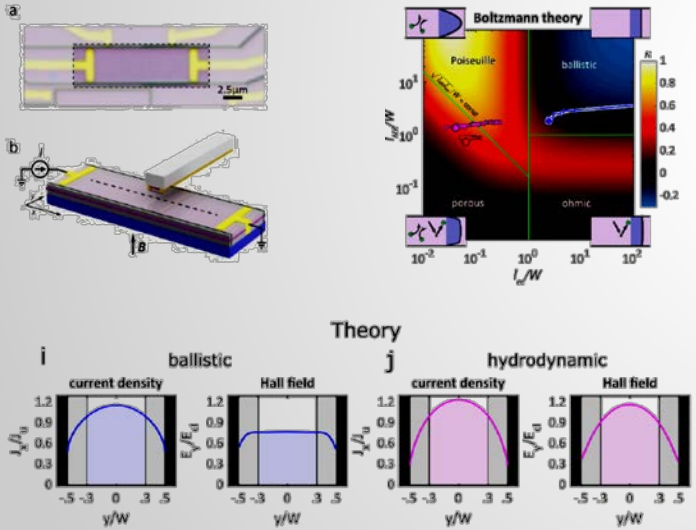

NV centers in diamonds – “Dirac fluid”

Harvard group (2020)

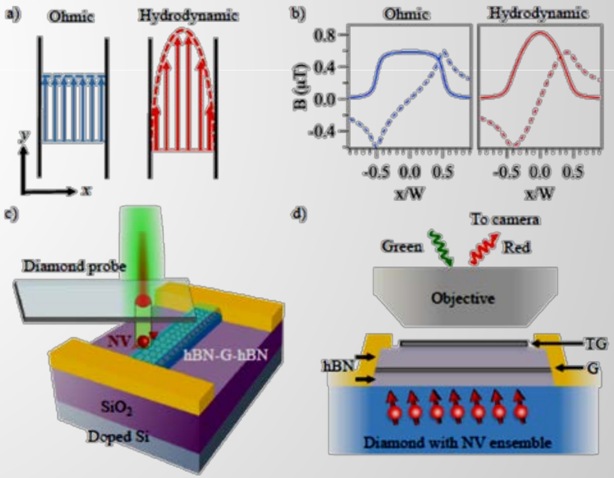

Poiseuille flow in doped graphene

nearly single-band electronic fluid is similar to conventional fluids and may exhibit Poiseuille-like flow

scanning nanotube SET – doped graphene

Weizmann group (2019)

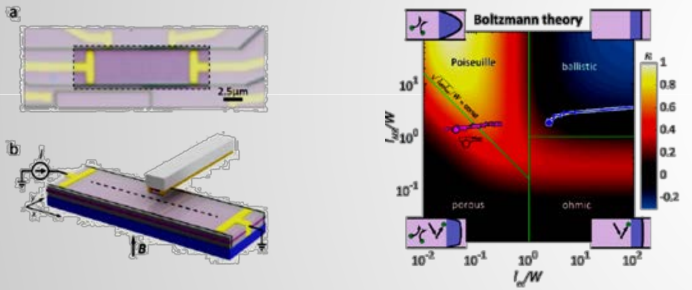

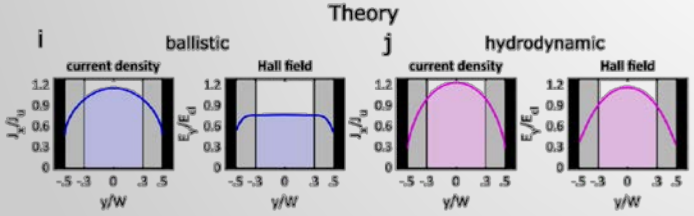

Poiseuille-like flow – catenary flow profile

Alekseev et.al (2018)

current density with no-slip boundary conditions

$$J_x = \sigma E_x \left[1 - \frac{\cosh(y/\ell_G)}{\cosh[W/(2\ell_G)]} \right]$$

Gurzhi length

$$\ell_G = \sqrt{\nu \tau_{\text{dis}}}$$

Scaffidi et. al (2017); Pellegrino, Torre, Polini (2017);
Alekseev et.al (2018)

no-slip boundary conditions are unrealistic, but mixed (Maxwell's) boundary conditions lead to similar bulk behavior

Kiselev, Schmalian (2019)

viscosity in graphene in the degenerate regime

model calculation yields good qualitative agreement with the data but overestimates the value

data from nonlocal transport

Geim group (2016)

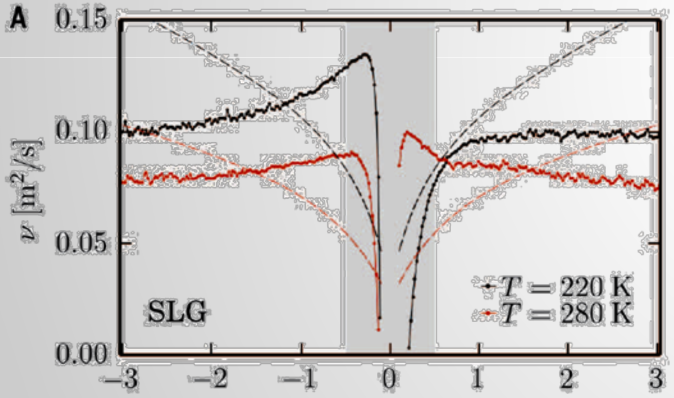

three-mode approximation

Schütt, BN (2019)

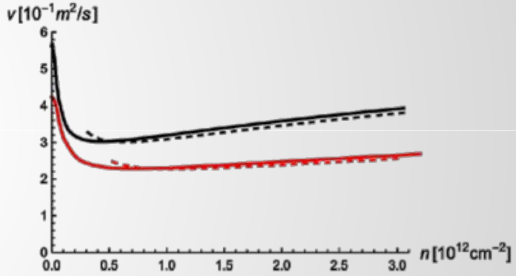

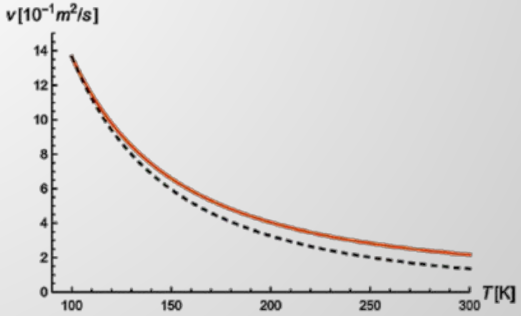

viscosity in graphene near charge neutrality

Schütt, BN (2019)

hydrodynamics at charge neutrality

electric current

$$\boldsymbol{j} = n\boldsymbol{u} + \delta\boldsymbol{j} = \delta\boldsymbol{j}$$

generalized Stokes (linear) equation

$$\boldsymbol{\nabla} P = \eta \Delta \boldsymbol{u} + \frac{e}{c}\delta\boldsymbol{j} \times \boldsymbol{B} - \frac{3P\boldsymbol{u}}{v_g^2 \tau_{\mathrm{dis}}}$$

in the absence of magnetic field, the electric current in neutral graphene is not hydrodynamic

BN, Gornyi, Titov (2021)

understanding of boundary conditions is key to interpret experimental data: channel geometry does not support Poiseuille flow!

viscosity at arbitrary densities

Harvard group (2020)

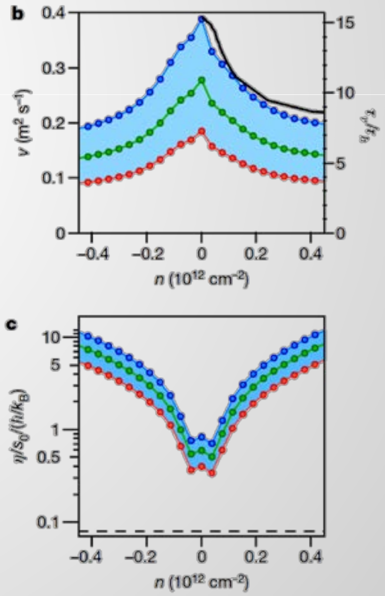

Wiedemann-Franz law violation

observed in graphene and topological materials

Wiedemann-Franz law violation

measured Lorenz number in the hydrodynamic regime significantly deviates from the universal (FL) value

experiment in graphene

Kim group (2016)

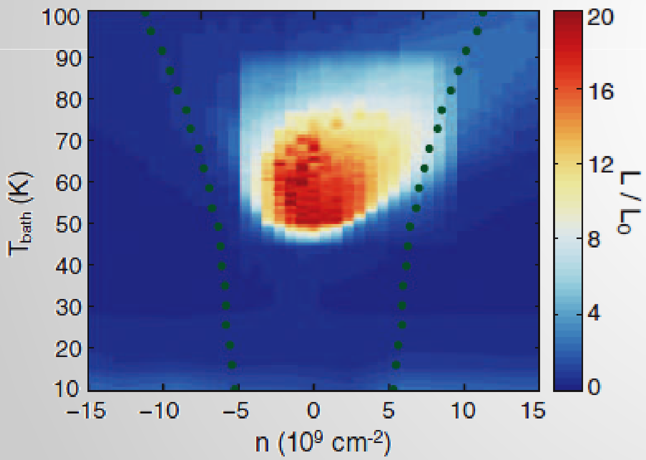

topological materials (WP_2, MoP)

Felser group (2018)

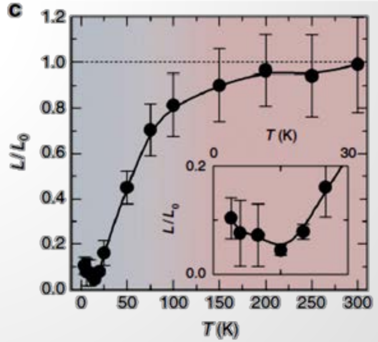

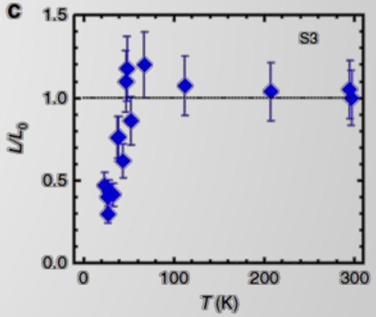

“disorder-assisted” Wiedemann-Franz law

artificially introduced disorder (by means of irradiation) restores the Wiedemann-Franz law in VO_2, the strongly correlated metal with resistivity exceeding the Mott-Ioffe-Regel limit (at high temperatures T>341 K)

VO_2 nanowire irradiated with He

Berkeley group (2020)

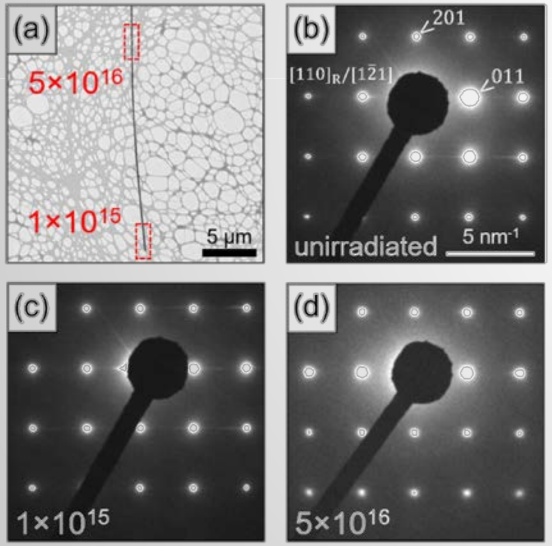

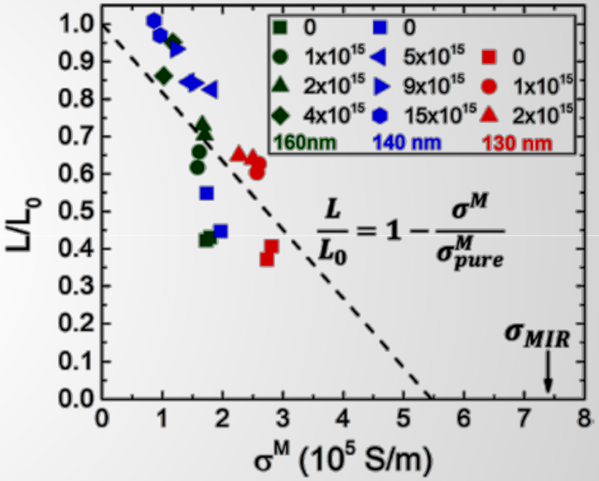

FIG. 3. Normalized Lorenz number L/L_0 [as defined in Eq. (1)] for three VO_2 nanowires of different thicknesses (labeled) for different irradiation doses (in units of ions/cm^2) as a function of σ for the M phase just above the MIT, showing the recovery of L upon introduction of defects toward the Sommerfeld value ($L_0 = 2.44 \times 10^{-8}\ \mathrm{W\,\Omega\,K^{-2}}$) of a normal metal. The error range of the L/L_0 data points is about ±0.1. The MIR limit of σ is indicated with an arrow, proving that all data exceed the σ_{MIR}.

lecture 11: microscopic "derivation"

traditional hydrodynamics

Google Search

I'm Feeling Lucky

Galilean-invariant fluids

Landau, Lifshitz, vols. 6, 10

continuity equations

conservation of the number of particles

$$\partial_t \rho + \boldsymbol{\nabla} \rho \langle \boldsymbol{v} \rangle = 0$$

conservation of energy

$$\partial_t N \langle \epsilon \rangle + \boldsymbol{\nabla} \boldsymbol{j}_E = 0$$

momentum conservation

$$\partial_t \rho \langle v_\alpha \rangle + \partial_\beta \Pi_{\alpha\beta} = 0$$

ideal fluid hydrodynamics

Euler equation (1755)

$$\frac{d\boldsymbol{v}}{dt} \equiv \frac{\partial \boldsymbol{v}}{\partial t} + (\boldsymbol{v} \cdot \boldsymbol{\nabla})\, \boldsymbol{v} = -\frac{1}{\rho} \boldsymbol{\nabla} p$$

mechanics of continuum medium:

a small "element" contains macroscopic number of constituent atoms or molecules

Newtonian equation of motion

slow varying macroscopic quantities

adiabatic flow (entropy is conserved)

Galilean-invariant fluids

Landau, Lifshitz, vols. 6, 10

continuity equations

conservation of the number of particles

$$\partial_t \rho + \boldsymbol{\nabla} \rho \langle \boldsymbol{v} \rangle = 0$$

conservation of energy

$$\partial_t N \langle \epsilon \rangle + \boldsymbol{\nabla} \boldsymbol{j}_E = 0$$

momentum conservation

$$\partial_t \rho \langle v_\alpha \rangle + \partial_\beta \Pi_{\alpha\beta} = 0$$

ideal fluid hydrodynamics

Euler equation (1755)

$$\frac{d\boldsymbol{v}}{dt} \equiv \frac{\partial \boldsymbol{v}}{\partial t} + (\boldsymbol{v} \cdot \boldsymbol{\nabla})\, \boldsymbol{v} = -\frac{1}{\rho} \boldsymbol{\nabla} p$$

stress tensor

$$\Pi_{\alpha\beta} = p\delta_{\alpha\beta} + \rho v_\alpha v_\beta$$

energy current

$$\boldsymbol{j}_E = \rho \boldsymbol{v} \left(\frac{v^2}{2} + w \right)$$

Galilean-invariant fluids

Landau, Lifshitz, vols. 6, 10

dissipative corrections

stress tensor

$$\Pi_{\alpha\beta} = p\delta_{\alpha\beta} + \rho v_\alpha v_\beta - \sigma'_{\alpha\beta}$$

isotropic fluid

$$\sigma'_{\alpha\beta} = \eta\left[\partial_\alpha v_\beta + \partial_\beta v_\alpha - \frac{2}{3}\delta_{\alpha\beta}\boldsymbol{\nabla}\cdot\boldsymbol{v}\right] + \zeta\delta_{\alpha\beta}\boldsymbol{\nabla}\cdot\boldsymbol{v}$$

energy current

$$j_E^\alpha = \rho v_\alpha\left(\frac{v^2}{2} + w\right) - v_\beta\sigma'_{\beta\alpha} - \varkappa\nabla_\alpha T$$

viscous hydrodynamics

Navier (1827), Stokes (1845)

$$\rho\left[\frac{\partial\boldsymbol{v}}{\partial t} + (\boldsymbol{v}\cdot\boldsymbol{\nabla})\,\boldsymbol{v}\right] = -\boldsymbol{\nabla}p + \eta\Delta\boldsymbol{v} + \left[\zeta + \frac{\eta}{3}\right]\boldsymbol{\nabla}(\boldsymbol{\nabla}\cdot\boldsymbol{v})$$

incompressible fluid

$$\frac{\partial\boldsymbol{v}}{\partial t} + (\boldsymbol{v}\cdot\boldsymbol{\nabla})\,\boldsymbol{v} = -\frac{1}{\rho}\boldsymbol{\nabla}p + \frac{\eta}{\rho}\Delta\boldsymbol{v}$$

$$\nu = \eta/\rho$$

$$R = ul/\nu$$

heat transport

$$\rho T\left(\frac{\partial s}{\partial t} + \boldsymbol{v}\boldsymbol{\nabla}s\right) = \sigma'_{\alpha\beta}\frac{\partial v_\alpha}{\partial x_\beta} + \boldsymbol{\nabla}\cdot(\varkappa\boldsymbol{\nabla}T)$$

Galilean-invariant fluids

Landau, Lifshitz, vols. 6, 10

Poiseuille flow

Poiseuille (1840)

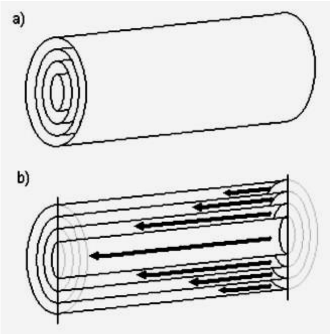

$$\nabla p = \eta \Delta \boldsymbol{v}$$

$$u_z = -\frac{\partial p}{\partial z}\frac{R^2 - r^2}{4\eta}$$

$$u_r = u_\theta = 0$$

$$I = \frac{\pi n R^4}{8\eta l}\delta p$$

incompressible fluid

no-slip boundary conditions

parabolic velocity profile

Poiseuille flow in the presence of obstacles

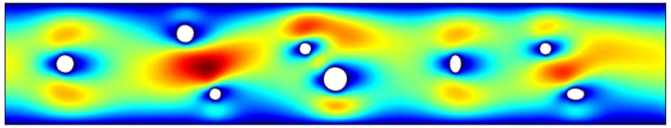

flows around obstacles avoiding scattering

flow rate exceeding independent molecular flow (Knudsen flow)

key to understand superballistic transport experiments in graphene

kinetic theory and “derivation” of hydrodynamics

Boltzmann equation (no external fields)

Landau, Lifshitz, vol. 10

Boltzmann equation

$$\mathcal{L} f_\lambda = \mathrm{St}[f_\lambda]$$

$$\mathcal{L} = \partial_t + \boldsymbol{v} \cdot \boldsymbol{\nabla}_{\boldsymbol{r}}$$

local equilibrium distribution function

$$\mathrm{St}[f_\lambda^{(0)}] = 0$$

macroscopic quantities

$$\rho = \sum_\lambda f_\lambda$$

$$\rho \langle \boldsymbol{v} \rangle = \sum_\lambda \boldsymbol{v} f_\lambda$$

$$N \langle \epsilon \rangle = \sum_\lambda \epsilon_\lambda f_\lambda$$

$$\boldsymbol{j}_E = \sum_\lambda \boldsymbol{v} \epsilon_\lambda f_\lambda$$

$$\Pi_{\alpha\beta} = \sum_\lambda v_\alpha v_\beta f_\lambda$$

conservation laws

Landau, Lifshitz, vols. 6, 10

conservation laws

conservation of the number of particles

$$\sum_\lambda \mathrm{St}[f_\lambda] = 0$$

conservation of energy

$$\sum_\lambda \epsilon_\lambda \mathrm{St}[f_\lambda] = 0$$

momentum conservation

$$\sum_\lambda \boldsymbol{p}\,\mathrm{St}[f_\lambda] = 0, \qquad \boldsymbol{p} = m\boldsymbol{v}$$

continuity equations

conservation of the number of particles

$$\partial_t \rho + \boldsymbol{\nabla} \rho \langle \boldsymbol{v} \rangle = 0$$

conservation of energy

$$\partial_t N \langle \epsilon \rangle + \boldsymbol{\nabla} \boldsymbol{j}_E = 0$$

momentum conservation

$$\partial_t \rho \langle v_\alpha \rangle + \partial_\beta \Pi_{\alpha\beta} = 0$$

viscous fluids

Landau, Lifshitz, vols. 6, 10

dissipative corrections

stress tensor

$$\Pi_{\alpha\beta} = \Pi^{(0)}_{\alpha\beta} + \delta\Pi_{\alpha\beta} = p\delta_{\alpha\beta} + \rho v_\alpha v_\beta - \sigma'_{\alpha\beta}$$

isotropic fluid

$$\sigma'_{\alpha\beta} = \eta\left[\partial_\alpha v_\beta + \partial_\beta v_\alpha - \frac{2}{3}\delta_{\alpha\beta}\boldsymbol{\nabla}\cdot\boldsymbol{v}\right] + \zeta\delta_{\alpha\beta}\boldsymbol{\nabla}\cdot\boldsymbol{v}$$

energy current

$$j_E^\alpha = j_{E,0}^\alpha + \delta j_E^\alpha = \rho v_\alpha\left(\frac{v^2}{2} + w\right) - v_\beta\sigma'_{\beta\alpha} - \varkappa\nabla_\alpha T$$

viscous hydrodynamics

Navier (1827), Stokes (1845)

$$\rho\left[\frac{\partial\boldsymbol{v}}{\partial t} + (\boldsymbol{v}\cdot\boldsymbol{\nabla})\,\boldsymbol{v}\right] = -\boldsymbol{\nabla}p + \eta\Delta\boldsymbol{v} + \left[\zeta + \frac{\eta}{3}\right]\boldsymbol{\nabla}(\boldsymbol{\nabla}\cdot\boldsymbol{v})$$

incompressible fluid

$$\frac{\partial\boldsymbol{v}}{\partial t} + (\boldsymbol{v}\cdot\boldsymbol{\nabla})\,\boldsymbol{v} = -\frac{1}{\rho}\boldsymbol{\nabla}p + \nu\Delta\boldsymbol{v}$$

heat transport

$$\rho T\left(\frac{\partial s}{\partial t} + \boldsymbol{v}\boldsymbol{\nabla}s\right) = \sigma'_{\alpha\beta}\frac{\partial v_\alpha}{\partial x_\beta} + \boldsymbol{\nabla}\cdot(\varkappa\boldsymbol{\nabla}T)$$

unconventional hydrodynamics in graphene

recent review: BN, La Rivista del Nuovo Cimento **45**, 661 (2022)

hydrodynamic approach to graphene

Briskot et.al (2015), Schütt, BN (2019)

Dirac fermions in graphene

linear spectrum

no Galilean invariance

momentum density proportional to energy current

classical (3D) Coulomb interaction

no Lorentz invariance

Vlasov-like self-consistency

non-degenerate Fermi gas
(close to the neutrality point)

temperature is the only energy scale

transition to a Fermi-liquid-like behavior at high carrier densities

continuity equations

particle number (*two bands!*)

$$\partial_t n + \boldsymbol{\nabla} \cdot \boldsymbol{j} = 0$$

$$\partial_t n_I + \boldsymbol{\nabla} \cdot \boldsymbol{j}_I = -\left[n_I - n_I^{(0)}\right] / \tau_R$$

energy density

$$\partial_t n_E + \boldsymbol{\nabla} \cdot \boldsymbol{j}_E = e\boldsymbol{E} \cdot \boldsymbol{j} - \left[n_E - n_{E,0}\right] / \tau_{RE}$$

momentum density

$$\partial_t n_{\boldsymbol{k}}^\alpha + \nabla_{\boldsymbol{r}}^\beta \Pi_E^{\alpha\beta} - enE^\alpha - \frac{e}{c}\left[\boldsymbol{j} \times \boldsymbol{B}\right]^\alpha = -\frac{n_{\boldsymbol{k}}^\alpha}{\tau_{\text{dis}}}$$

$$\boldsymbol{j}_E = v_g^2 \boldsymbol{n}_{\boldsymbol{k}}$$

hydrodynamic approach to graphene

Briskot et.al (2015), Schütt, BN (2019)

Dirac fermions in graphene

linear spectrum

no Galilean invariance

momentum density proportional to energy current

classical (3D) Coulomb interaction

no Lorentz invariance

Vlasov-like self-consistency

non-degenerate Fermi gas
(close to the neutrality point)

temperature is the only energy scale

transition to a Fermi-liquid-like behavior at high carrier densities

continuity equations

particle number (*two bands!*)

$$\partial_t n + \boldsymbol{\nabla} \cdot \boldsymbol{j} = 0$$

$$\partial_t n_I + \boldsymbol{\nabla} \cdot \boldsymbol{j}_I = -\left[n_I - n_I^{(0)}\right] / \tau_R$$

energy density

$$\partial_t n_E + \boldsymbol{\nabla} \cdot \boldsymbol{j}_E = e\boldsymbol{E} \cdot \boldsymbol{j} - \left[n_E - n_{E,0}\right] / \tau_{RE}$$

momentum density

$$\partial_t n_{\boldsymbol{k}}^\alpha + \nabla_{\boldsymbol{r}}^\beta \Pi_E^{\alpha\beta} - enE^\alpha - \frac{e}{c}\left[\boldsymbol{j} \times \boldsymbol{B}\right]^\alpha = -\frac{n_{\boldsymbol{k}}^\alpha}{\tau_{\text{dis}}}$$

$$\boldsymbol{j}_E = v_g^2 \boldsymbol{n}_{\boldsymbol{k}}$$

ideal hydrodynamics in graphene

Briskot et.al (2015), Schütt, BN (2019)

does not rely on either Galilean or Lorentz invariance

local equilibrium

$$\mathrm{St} = \mathrm{St}_{ee} + \mathrm{St}_R + \mathrm{St}_{\mathrm{dis}}$$

local equilibrium distribution function

$$f^{(0)}_{\lambda,\boldsymbol{k}} = \frac{1}{1+\exp\left\{\left[\epsilon_{\lambda,\boldsymbol{k}} - \mu_\lambda(\boldsymbol{r}) - \boldsymbol{u}(\boldsymbol{r})\cdot\boldsymbol{k}\right]/T(\boldsymbol{r})\right\}}$$

thermodynamic quantities

$$P = n_E \frac{1-u^2/v_g^2}{2+u^2/v_g^2}$$

$$W = n_E + P = \frac{3n_E}{2+u^2/v_g^2}$$

hydrodynamic quantities

macroscopic currents

$$\boldsymbol{j}_E = W\boldsymbol{u}$$

$$\boldsymbol{j} = n\boldsymbol{u}$$

$$\boldsymbol{j}_I = n_I\boldsymbol{u}$$

stress-energy tensor

$$\Pi^E_{\alpha\beta} = \frac{n_E}{2+u^2}\left[\delta_{\alpha\beta}(1-u^2) + 3u_\alpha u_\beta\right]$$

ideal hydrodynamics in graphene

Briskot et.al (2015), Schütt, BN (2019)

does not rely on either Galilean or Lorentz invariance

local equilibrium

$$\mathrm{St} = \mathrm{St}_{ee} + \mathrm{St}_R + \mathrm{St}_{\mathrm{dis}}$$

local equilibrium distribution function

$$f^{(0)}_{\lambda,\boldsymbol{k}} = \frac{1}{1+\exp\left\{\left[\epsilon_{\lambda,\boldsymbol{k}} - \mu_\lambda(\boldsymbol{r}) - \boldsymbol{u}(\boldsymbol{r})\cdot\boldsymbol{k}\right]/T(\boldsymbol{r})\right\}}$$

thermodynamic quantities

$$P = n_E \frac{1-u^2/v_g^2}{2+u^2/v_g^2}$$

$$W = n_E + P = \frac{3n_E}{2+u^2/v_g^2}$$

collision integrals

$$N\sum_\lambda \int \frac{d^2k}{(2\pi)^2} \boldsymbol{k}\,\mathrm{St}_{\mathrm{dis}}[f_{\lambda\boldsymbol{k}}] = \frac{\boldsymbol{n_k}}{\tau_{\mathrm{dis}}}$$

$$N\sum_\lambda \int \frac{d^2k}{(2\pi)^2} \lambda\,\mathrm{St}_R[f_{\lambda\boldsymbol{k}}] \approx -\mu_I n_{I,0}\lambda_Q \approx -\frac{n_I - n_{I,0}}{\tau_R}$$

$$N\sum_{\boldsymbol{k}} \epsilon_{\lambda\boldsymbol{k}}\mathrm{St}_R[f_{\lambda\boldsymbol{k}}] = -\mu_I n_{E,0}\lambda_{QE} \approx -\frac{n_E - n_{E,0}}{\tau_{RE}}$$

ideal hydrodynamics in graphene

Briskot et.al (2015), Schütt, BN (2019)

generalized Euler equation

$$W(\partial_t + \boldsymbol{u}\cdot\boldsymbol{\nabla})\boldsymbol{u} + v_g^2\boldsymbol{\nabla}P + \boldsymbol{u}\partial_t P + e(\boldsymbol{E}\cdot\boldsymbol{j})\boldsymbol{u} = v_g^2 en\boldsymbol{E} + v_g^2\frac{e}{c}\boldsymbol{j}\times\boldsymbol{B} - \frac{W\boldsymbol{u}}{\tau_{\rm dis}}$$

linear response in degenerate limit

$$v_g^2 en\boldsymbol{E} + v_g^2\frac{e}{c}\boldsymbol{j}\times\boldsymbol{B} = \frac{\mu\boldsymbol{j}}{\tau_{\rm dis}}$$

Drude-like resistivity

$$\rho_{xx}^{(0)} = \frac{\pi}{e^2|\mu|\tau_{\rm dis}} \qquad R_H^{(0)} = \frac{1}{nec}$$

charge-energy decoupling in neutral graphene

$$v_g^2\frac{e}{c}\boldsymbol{j}\times\boldsymbol{B} = \frac{\boldsymbol{j}_E}{\tau_{\rm dis}}$$

key to understand Wiedemann-Franz law violation in graphene

parabolic magnetoresistance

$$\delta R(B;\mu=0) = \mathcal{C}\frac{v_g^4}{c^2}\frac{B^2\tau_{\rm dis}}{T^3} \qquad R_H = 0$$

Müller, Sachdev (2008); BN et.al (2015)

dissipation and viscous hydrodynamics

dissipative terms in graphene

Briskot et.al (2015), Schütt, BN (2019)

dissipative parts of the currents

electrical and imbalance currents

$$\boldsymbol{j} = n\boldsymbol{u} + \delta\boldsymbol{j} \qquad \boldsymbol{j}_I = n_I\boldsymbol{u} + \delta\boldsymbol{j}_I$$

$$\begin{pmatrix} \delta\boldsymbol{j} \\ \delta\boldsymbol{j}_I \end{pmatrix} = \hat{\Sigma} \begin{pmatrix} e\boldsymbol{E} - T\boldsymbol{\nabla}(\mu/T) \\ -T\boldsymbol{\nabla}(\mu_I/T) \end{pmatrix}$$

conductivity at charge neutrality

$$\sigma_Q = e^2\Sigma_{11}(0) \qquad \Sigma_{12}(0) = 0$$

$$\sigma_Q = \mathcal{A}\,\frac{e^2}{\alpha_g^2} \qquad \mathcal{A} \approx 0.12$$

Kashuba (2008)

viscosity

dissipative part of the stress tensor

$$\delta\Pi^E_{\alpha\beta} = -\eta\left[\nabla_\alpha u_\beta + \nabla_\beta u_\alpha - \delta_{\alpha\beta}\boldsymbol{\nabla}\cdot\boldsymbol{u}\right]$$

zero bulk viscosity

$$\zeta = 0$$

viscosity near charge neutrality

Müller et.al, (2009)

$$\eta(\mu = 0) = \mathcal{B}\,\frac{T^2}{\alpha_g^2 v_g^2} \qquad \mathcal{B} \approx 0.45$$

viscosity: formal definitions

Read, Rezayi (2011), Bradlyn, Goldstein, Read (2012), Link, Sheehy, BN, Schmalian (2017)

viscous stress tensor

first-order gradient expansion

$$\delta\Pi_{\alpha\beta} = \sum_{\gamma\delta} \eta_{\alpha\beta\gamma\delta} \frac{\partial v_\delta}{\partial x_\gamma}$$

rotational invariance

$$\delta\Pi_{\alpha\beta} = \eta\left(\frac{\partial u_\alpha}{\partial x_\beta} + \frac{\partial u_\beta}{\partial x_\alpha} - \frac{2}{d}\delta_{\alpha\beta}\boldsymbol{\nabla}\cdot\boldsymbol{u}\right) + \zeta\delta_{\alpha\beta}\boldsymbol{\nabla}\cdot\boldsymbol{u}$$

shear viscosity (with rotational invariance)

$$\eta_{\alpha\beta\gamma\delta} = \eta\left(\delta_{\alpha\gamma}\delta_{\beta\delta} + \delta_{\alpha\delta}\delta_{\beta\gamma} - \frac{2}{d}\delta_{\alpha\beta}\delta_{\gamma\delta}]\right)$$

stress tensor and strain generators

$$\delta\Pi_{\alpha\beta}x_\beta = -i\,[H, \mathcal{J}_{\alpha\beta}]$$

Kubo formula for viscosity

$$\eta_{\alpha\beta\delta\gamma} = -i\,\langle[\mathcal{J}_{\alpha\beta}(0), \mathcal{J}_{\gamma\delta}(0)]\rangle + \\ +\omega_+ \int_0^\infty dt + \langle[\mathcal{J}_{\alpha\beta}(0), \mathcal{J}_{\gamma\delta}(t)]\rangle\, e^{i\omega_+ t}$$

relation to conductivity

$$\sigma_{\nu\beta} = \frac{in}{m\omega_+}\delta_{\nu\beta} + \frac{q_\mu q_\alpha}{m^2\omega_+^2}\left(\eta_{\mu\nu\alpha\beta} + \frac{i}{\kappa\omega_+}\delta_{\mu\nu}\delta_{\alpha\beta}\right)$$

collinear scattering singularity (allows to solve the kinetic equation)

Kashuba (2008), Müller, Schmalian, Fritz (2009)

collinear scattering

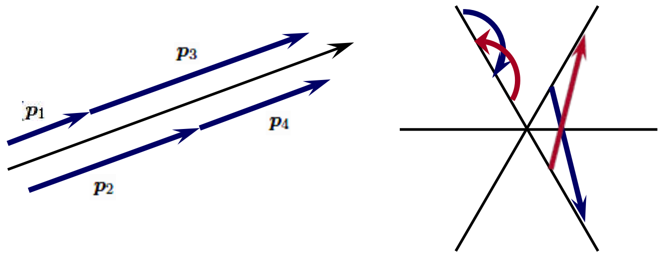

equivalence of energy and momentum conservation laws

$$\boldsymbol{p}_1 + \boldsymbol{p}_3 = \boldsymbol{p}_2 + \boldsymbol{p}_4$$

$$\epsilon_i = \pm v |\boldsymbol{p}_i|$$

$$\epsilon_1 + \epsilon_3 = \epsilon_2 + \epsilon_4$$

three macroscopic currents

formally divergent collision integral

$$"I_{ij} \sim \ln \alpha \gg 1"$$

three special modes

$$\delta f \propto \boldsymbol{p} \quad \Rightarrow \quad \mathcal{I} = 0$$

$$\delta f \propto \boldsymbol{v} \quad \Rightarrow \quad \mathcal{I} = 0 \qquad \text{if} \;\; \boldsymbol{v}_i \| \boldsymbol{v}_j$$

$$\delta f \propto \boldsymbol{v}\,\mathrm{sign}(\epsilon) \quad \Rightarrow \quad \mathcal{I} = 0 \qquad \text{if} \;\; \boldsymbol{v}_i \| \boldsymbol{v}_j$$

dissipative terms in graphene - viscosity

Briskot et.al (2015); Schütt, BN (2019)

viscosity in graphene

dissipative part of the stress tensor

$$\Pi_E^{\alpha\beta} = \Pi_{E,0}^{\alpha\beta} + \delta\Pi_E^{\alpha\beta},$$
$$\delta\Pi_E^{\alpha\beta} = -\eta(B)\mathfrak{D}^{\alpha\beta} + \eta_H(B)\epsilon^{\alpha ij}\mathfrak{D}^{i\beta}e_B^j,$$
$$\mathfrak{D}^{\alpha\beta} = \nabla^\alpha u^\beta + \nabla^\beta u^\alpha - \delta^{\alpha\beta}\nabla\cdot\boldsymbol{u},$$

zero bulk viscosity

$$\zeta = 0$$

viscosity near charge neutrality

Müller et.al, (2009)

$$\eta(\mu=0) = \mathcal{B}\,\frac{T^2}{\alpha_g^2 v_g^2} \qquad \mathcal{B}\approx 0.45$$

viscosity in magnetic field

shear viscosity

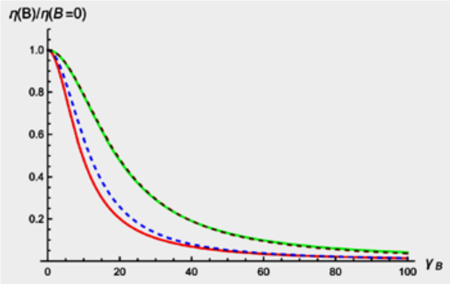

Hall viscosity

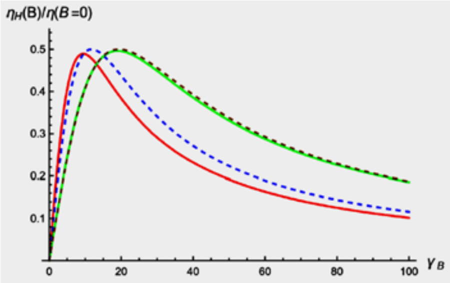

kinematic viscosity away from charge neutrality

Schütt, BN (2019)

kinematic viscosity

"diffusion-like" part of the Navier-Stokes equation

$$W\left[\partial_t - \frac{v_g^2\eta}{W}\nabla^2\right]\boldsymbol{u} + \cdots = 0$$

kinematic viscosity at charge neutrality

$$\nu(\mu\!=\!0) = \frac{v_g^2\eta}{W} = \frac{2\pi\mathcal{B}}{9\zeta(3)}\frac{v_g^2}{\alpha^2 T}$$

kinematic viscosity in degenerate regime

$$\nu(\mu\!\to\!\infty) = \frac{3}{128\pi}\frac{v_g^2\mu}{\alpha^2 T^2}\frac{1}{\ln}$$

Principi et.al (2016)

viscosity at arbitrary densities

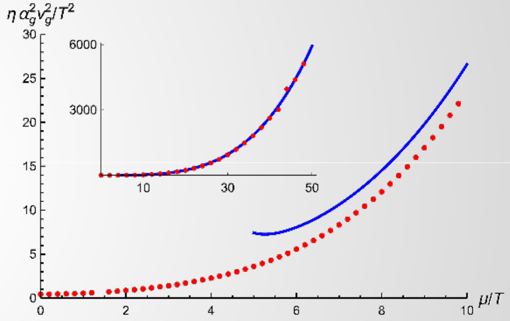

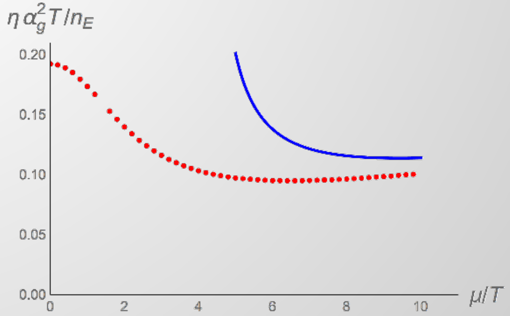

kinematic viscosity in the degenerate regime

Schütt, BN (2019)

kinematic viscosity

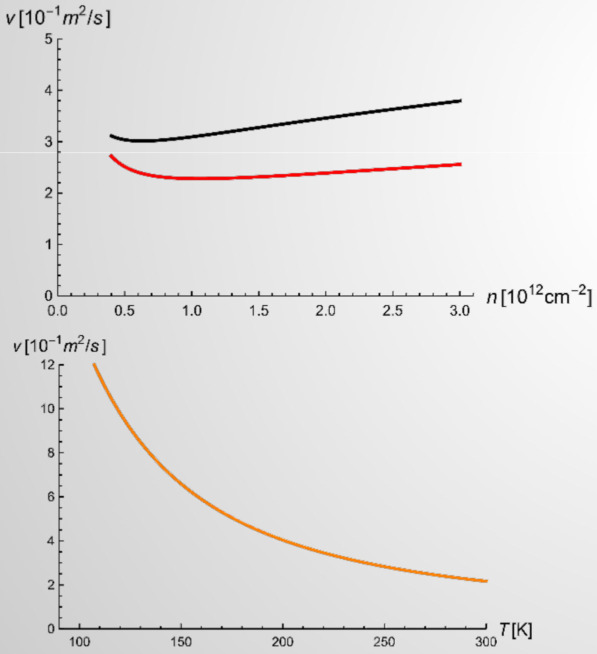

Hall viscosity

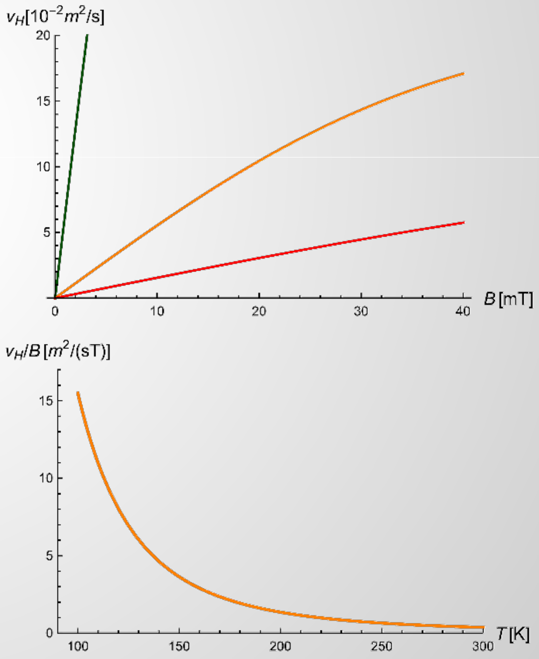

field-dependent viscosity

Schütt, BN (2019)

viscosity in degenerate limit

shear viscosity

$$\eta(B;\mu\gg T)=\frac{\eta(B=0;\mu\gg T)}{1+\Gamma_B^2}$$

Steinberg (1958)

Hall viscosity

$$\eta_H(B;\mu\gg T)=\eta(B=0;\mu\gg T)\frac{\Gamma_B}{1+\Gamma_B^2}$$

effective “cyclotron frequency”

$$\Gamma_B=2\omega_B\tilde{\tau}_{11},\quad \omega_B=\frac{|e|v_g^2B}{c\mu}$$

Alekseev (2016); Scaffidi et.al (2017)

“semiclassical” field dependence

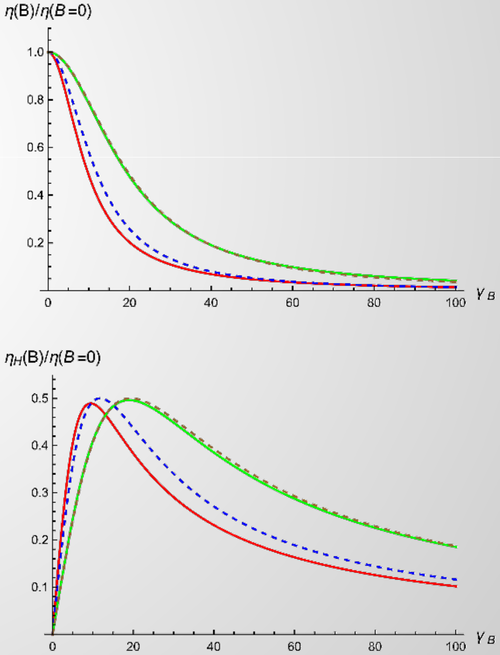

lower bound on viscosity

most known hydrodynamic systems are characterized by a viscosity to entropy density ratio that is larger than a certain universal value; this statement might not be literally applicable to anisotropic systems.

AdS/CFT correspondence

Kovtun, Son, Starinets (2005)

$$\frac{\eta}{s} \geqslant \frac{\hbar}{4\pi k_B}$$

uncertainty principle interpretation

$$\eta \propto \tau n_E, \qquad s \propto k_B n$$

$$\frac{\eta}{s} \propto \frac{\tau n_E}{k_B n} \gtrsim \frac{\hbar}{k_B}$$

anisotropic Dirac systems

Link, BN, Schmalian (2018)

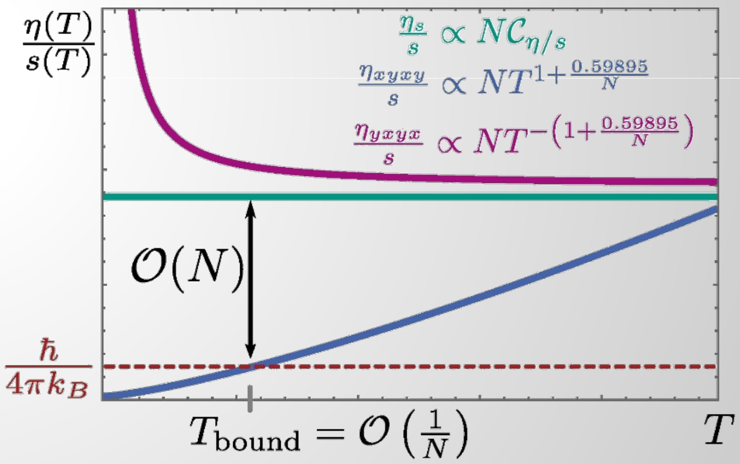

relation to relativistic hydrodynamics

relativistic hydrodynamics

Landau, Lifshitz, vol. 6

dissipative corrections

stress tensor

$$T_{ik} = pg_{ik} + wu_iu_k + \tau_{ik}$$

$$\tau_{ik} = -c\eta\left(\frac{\partial u_i}{\partial x^k} + \frac{\partial u_k}{\partial x^i} - u_k u^l \frac{\partial u_i}{\partial x^l} - u_i u^l \frac{\partial u_k}{\partial x^l}\right) -$$

$$-c\left(\zeta - \frac{2}{3}\eta\right)\frac{\partial u^l}{\partial x^l}(g_{ik} - u_i u_k)$$

current

$$j_i = nu_i + \nu_i$$

$$\nu_i = \frac{\varkappa}{c}\left(\frac{nT}{w}\right)^2\left[\frac{\partial}{\partial x^i}\frac{\mu}{T} - u_i u^k \frac{\partial}{\partial x^k}\frac{\mu}{T}\right]$$

equations of motion

$$\frac{\partial T_i^k}{\partial x^k} = 0 \qquad \frac{\partial j^i}{\partial x^i} = 0$$

ideal hydrodynamics

$$wu^k \frac{\partial u_i}{\partial x^k} = \frac{\partial p}{\partial x^i} - u_i u^k \frac{\partial p}{\partial x^k}$$

coupled energy and mass flows

hydrodynamic quantities are defined in the rest frame where the relation of energy to other thermodynamic quantities is unaffected by dissipation

$$\tau_{ik}u^k = 0 \qquad \nu_k u^k = 0$$

relativistic hydrodynamics

formal similarity between hydrodynamic equations in graphene and in relativistic theory; *relativistic hydrodynamics defines thermodynamic quantities in the rest frame; kinetic theory in graphene – in the co-moving frame*

hydrodynamic quantities

$$w = 3p$$

energy density

$$T^{00} = \frac{w}{1-u^2/v_g^2} - p \qquad n_E = \frac{3P}{1-u^2/v_g^2} - P$$

momentum density

$$T^{0\alpha} = \frac{wu_\alpha}{v_g(1-u^2/v_g^2)} \qquad \boldsymbol{n_k} = \frac{3P\boldsymbol{u}}{v_g^2(1-u^2/v_g^2)}$$

momentum flux density

$$T^{\alpha\beta} = \frac{wu_\alpha u_\beta}{v_g^2(1-u^2/v_g^2)} + p\delta_{\alpha\beta}$$

$$\Pi_E^{\alpha\beta} = P\delta_{\alpha\beta} + \frac{3Pu_\alpha u_\beta}{v_g^2(1-u^2/v_g^2)}$$

equations of motion

ideal hydrodynamics

$$\frac{w}{1-u^2/v_g^2}\left[\frac{\partial}{\partial t} + \boldsymbol{u}\cdot\boldsymbol{\nabla}\right]\boldsymbol{u} + v_g^2\boldsymbol{\nabla}p + \boldsymbol{u}\frac{\partial p}{\partial t} = 0$$

$$W = \frac{3P}{1-u^2/v_g^2}$$

dissipative corrections (non-relativistic limit)

$$\tau_{\alpha\beta} \to \eta\left(\nabla_\alpha u^\beta + \nabla_\beta u^\alpha - \delta_{\alpha\beta}\boldsymbol{\nabla}\cdot\boldsymbol{u}\right) + \zeta\delta_{\alpha\beta}\boldsymbol{\nabla}\cdot\boldsymbol{u}$$

$$\boldsymbol{\nu} = A\frac{u_0}{v_g T}e\boldsymbol{E}, \quad A = \frac{v_g}{e^2}T\sigma_Q$$

entropy flow: heat transfer equation

electronic entropy in graphene

BN, Gornyi (2021)

entropy

definition

$$s = N\sum_\lambda \int \frac{d^2k}{(2\pi)^2} \mathcal{S}[f_{\lambda\boldsymbol{k}}]$$

$$\mathcal{S}[f_{\lambda\boldsymbol{k}}] = -[f_{\lambda\boldsymbol{k}} \ln f_{\lambda\boldsymbol{k}} + (1-f_{\lambda\boldsymbol{k}})\ln(1-f_{\lambda\boldsymbol{k}})]$$

derivatives of entropy

$$\frac{\partial s}{\partial z} = N\sum_\lambda \int \frac{d^2k}{(2\pi)^2} \frac{\partial \mathcal{S}[f_{\lambda\boldsymbol{k}}]}{\partial f_{\lambda\boldsymbol{k}}} \frac{\partial f_{\lambda\boldsymbol{k}}}{\partial z}$$

entropy current

$$\boldsymbol{j}_S = N\sum_\lambda \int \frac{d^2k}{(2\pi)^2} \boldsymbol{v}_{\lambda\boldsymbol{k}} \mathcal{S}[f_{\lambda\boldsymbol{k}}]$$

heat transfer equation: ideal fluid

“continuity equation”

$$\frac{\partial s}{\partial t} + \boldsymbol{\nabla}_{\boldsymbol{r}} \cdot \boldsymbol{j}_S = \mathcal{I}$$

collision integral

$$\mathcal{I} = N\sum_\lambda \int \frac{d^2k}{(2\pi)^2} \frac{\partial \mathcal{S}[f_{\lambda\boldsymbol{k}}]}{\partial f_{\lambda\boldsymbol{k}}} (\mathrm{St}_{ee}[f] + \mathrm{St}_R[f] + \mathrm{St}_{\mathrm{dis}}[f])$$

$$\mathcal{I} = \frac{1}{T}\frac{n_E - n_{E,0}}{\tau_{RE}} + \frac{\mu_I}{T}\frac{n_I - n_{I,0}}{\tau_R} + \frac{\boldsymbol{u}\cdot\boldsymbol{n}_{\boldsymbol{k}}}{T\tau_{\mathrm{dis}}}$$

unconventional hydrodynamics in graphene

hydrodynamic equations in graphene

Briskot et.al (2015), Schütt, BN (2019), BN, Gornyi (2021)

generalized hydrodynamic equations

$$W(\partial_t + \boldsymbol{u}\cdot\boldsymbol{\nabla})\boldsymbol{u} + v_g^2\boldsymbol{\nabla}P + \boldsymbol{u}\partial_t P + e(\boldsymbol{E}\cdot\boldsymbol{j})\boldsymbol{u} = v_g^2\left[en\boldsymbol{E} + \frac{e}{c}\boldsymbol{j}\times\boldsymbol{B} + \eta\nabla^2\boldsymbol{u} + \eta_H\nabla^2\boldsymbol{u}\times\boldsymbol{e}_{\boldsymbol{B}}\right] - \frac{W\boldsymbol{u}}{\tau_{\text{dis}}}$$

$$T\left[\frac{\partial s}{\partial t} + \boldsymbol{\nabla}\cdot\left(s\boldsymbol{u} - \delta\boldsymbol{j}\frac{\mu}{T} - \delta\boldsymbol{j}_I\frac{\mu_I}{T}\right)\right] = \delta\boldsymbol{j}\cdot\left[e\boldsymbol{E} + \frac{e}{c}\boldsymbol{u}\times\boldsymbol{B} - T\boldsymbol{\nabla}\frac{\mu}{T}\right] -$$

$$-T\delta\boldsymbol{j}_I\cdot\boldsymbol{\nabla}\frac{\mu_I}{T} + \frac{\eta}{2}\left(\nabla^\alpha u^\beta + \nabla^\beta u^\alpha - \delta^{\alpha\beta}\boldsymbol{\nabla}\cdot\boldsymbol{u}\right)^2 - \frac{n_E - n_{E,0}}{\tau_{RE}} + \mu_I\frac{n_I - n_{I,0}}{\tau_R} + \frac{\mathcal{W}\boldsymbol{u}^2}{v_g^2\tau_{\text{dis}}}.$$

continuity equations

$$\partial_t n + \boldsymbol{\nabla}\cdot\boldsymbol{j} = 0$$

$$\partial_t n_I + \boldsymbol{\nabla}\cdot\boldsymbol{j}_I = -\left[n_I - n_I^{(0)}\right]/\tau_R$$

equations of state

$$P = \frac{(1-u^2)n_E}{2+u^2}$$

$$W = \frac{2w}{2+u^2}, \quad w = n_E + P = 3n_E/2$$

plus Vlasov self-consistency and expressions for $\delta\boldsymbol{j},\ \delta\boldsymbol{j}_I$

lecture III: known solutions to hydrodynamic equations

hydrodynamic collective modes in graphene

independent variables

BN, Gornyi, Titov (2021)

equilibrium values of the variables

currents and external fields

$$\boldsymbol{j} = \boldsymbol{j}_I = \boldsymbol{j}_E = 0$$

$$\varphi = \bar{\varphi}, \qquad \boldsymbol{E} = -\boldsymbol{\nabla}\bar{\varphi} = 0$$

thermodynamic quantities

$$P = \bar{P} = \frac{N\bar{T}^3}{2\pi v_g^2}\tilde{n}_E \qquad W = 3\bar{P} \qquad s = \frac{3\bar{P} - \bar{\mu}\bar{n}}{\bar{T}}$$

$$n = \bar{n} = \frac{N\bar{T}^2}{2\pi v_g^2}\tilde{n}, \qquad n_I = \bar{n}_I = \frac{N\bar{T}^2}{2\pi v_g^2}\tilde{n}_I$$

$$\mu = \bar{\mu}, \qquad T = \bar{T}, \qquad \mu_I = 0, \qquad x = \bar{\mu}/\bar{T}$$

choice of variables

inhomogeneous fluctuations

$$\mu = \bar{\mu} + \delta\mu \qquad T = \bar{T} + \delta T \qquad \varphi = \bar{\varphi} + \delta\varphi$$

$$n = \bar{n} + \delta n \qquad n_I = \bar{n}_I + \delta n_I \qquad P = \bar{P} + \delta P$$

not all variables are independent

variable choice 1

$$\delta n, \quad \delta n_I, \quad \delta P$$

variable choice 2

$$\delta T, \quad \mu_I, \quad \delta\zeta$$

$$\delta\zeta = \delta\varphi + \frac{1}{e}\delta\mu$$

electrochemical potential

linearized hydrodynamic equations

BN, Gornyi, Titov (2021)

linearized equations

$$\frac{3\bar{P}}{v_g^2}\partial_t \boldsymbol{u} + \boldsymbol{\nabla}\delta P = \eta\Delta\boldsymbol{u} + e\bar{n}\boldsymbol{E} - \frac{3\bar{P}\boldsymbol{u}}{v_g^2\tau_{\rm dis}}$$

$$\partial_t\delta n + \bar{n}\boldsymbol{\nabla}\cdot\boldsymbol{u} + \boldsymbol{\nabla}\cdot\delta\boldsymbol{j} = 0$$

$$\partial_t\delta n_I + \bar{n}_I\boldsymbol{\nabla}\cdot\boldsymbol{u} + \boldsymbol{\nabla}\cdot\delta\boldsymbol{j}_I = -\frac{\delta n_I}{\tau_R}$$

$$2\partial_t\delta P + 3\bar{P}\boldsymbol{\nabla}\cdot\boldsymbol{u} = -\frac{2\delta P}{\tau_{RE}}$$

dissipative corrections to currents

$$\begin{pmatrix}\delta\boldsymbol{j}\\ \delta\boldsymbol{j}_I\end{pmatrix} = \widehat{\Sigma}\begin{pmatrix}e\boldsymbol{E}\\ 0\end{pmatrix} - \frac{\bar{T}^2}{\mathcal{T}}\widehat{\Sigma}'\begin{pmatrix}\boldsymbol{\nabla}\delta\tilde{n} - \frac{2\tilde{n}}{3\tilde{n}_E}\boldsymbol{\nabla}\delta\tilde{n}_E\\ \boldsymbol{\nabla}\delta\tilde{n}_I - \frac{2\tilde{n}_I}{3\tilde{n}_E}\boldsymbol{\nabla}\delta\tilde{n}_E\end{pmatrix}$$

$$\frac{\partial\bar{n}}{\partial\bar{\mu}} = \frac{N\mathcal{T}}{2\pi v_g^2}, \qquad \mathcal{T} = 2\bar{T}\ln 2\cosh\frac{\bar{\mu}}{2\bar{T}}$$

collective modes

five equations, five variables

$$\boldsymbol{u}, \quad \delta n, \quad \delta n_I, \quad \delta P$$

transform into algebraic equations

$$\boldsymbol{u}(t,\boldsymbol{r}) = \int\frac{d\omega d\boldsymbol{q}}{(2\pi)^3}e^{-i\omega t + i\boldsymbol{q}\boldsymbol{r}}\boldsymbol{u}(\omega,\boldsymbol{q})$$

Vlasov self-consistency

$$V_s(\boldsymbol{q}) = \begin{cases} e/C, & \text{gated},\\ 2\pi e/q, & \text{Coulomb}.\end{cases}$$

collective modes in neutral graphene

BN, Gornyi, Titov (2021)

dimensionless linearized equations

$$\tilde{\boldsymbol{q}}\delta\tilde{n}_E - \frac{9\zeta(3)}{2}\left(\tilde{\omega}+i\frac{1+\tilde{q}^2\tilde{\ell}_G^2}{\tilde{\tau}_{\rm dis}}\right)\mathbf{v} = 0$$

$$\left(\tilde{\omega} + i\frac{2\pi\tilde{q}^2\sigma_0}{e^2N\ln 2}\right)\delta\tilde{n} = \frac{2\pi\sigma_0}{eN}\tilde{\boldsymbol{q}}\cdot\boldsymbol{\mathcal{E}}$$

$$\left(\tilde{\omega}+\frac{i}{\tilde{\tau}_R}+\frac{i2\pi\tilde{q}^2\sigma_I}{e^2N\ln 2}\right)\delta\tilde{n}_I - \frac{\pi^2}{6}\tilde{\boldsymbol{q}}\cdot\mathbf{v} - \frac{i4\pi^3\tilde{q}^2\sigma_I\delta\tilde{n}_E}{27\zeta(3)Ne^2\ln 2} = 0$$

$$2\left(\tilde{\omega}+\frac{i}{\tilde{\tau}_{RE}}\right)\delta\tilde{n}_E - \frac{9\zeta(3)}{2}\tilde{\boldsymbol{q}}\cdot\mathbf{v} = 0$$

dissipative corrections to currents

$$\delta\tilde{\boldsymbol{j}} = \frac{1}{e}\sigma_0\boldsymbol{\mathcal{E}} - \frac{i\tilde{\boldsymbol{q}}\sigma_0}{e^2\ln 2}\delta\tilde{n}$$

$$\delta\tilde{\boldsymbol{j}}_I = -\frac{i\tilde{\boldsymbol{q}}\sigma_I}{e^2\ln 2}\left(\delta\tilde{n}_I - \frac{2\pi^2}{27\zeta(3)}\delta\tilde{n}_E\right)$$

collective modes

energy mode

$$\tilde{\omega} = \sqrt{\frac{\tilde{q}^2}{2} - \frac{1}{4}\left[\frac{1+\tilde{q}^2\tilde{\ell}_G^2}{\tilde{\tau}_{\rm dis}} - \frac{1}{\tilde{\tau}_{RE}}\right]^2} - i\frac{1+\tilde{q}^2\tilde{\ell}_G^2}{2\tilde{\tau}_{\rm dis}} - \frac{i}{2\tilde{\tau}_{RE}}$$

charge mode

$$\omega = -iD_0q^2\left[1+eV_s(q)\frac{\partial n}{\partial\mu}\right], \qquad D_0 = \frac{1}{2}\frac{v_g^2\tau_{11}\tau_{\rm dis}}{\tau_{11}+\tau_{\rm dis}}$$

imbalance mode

$$\omega = -iD_Iq^2 - \frac{i}{\tau_R}, \qquad D_I = \frac{1}{2}\frac{v_g^2\tau_{22}\tau_{\rm dis}\delta_I}{\tau_{22}\delta_I+\tau_{\rm dis}}$$

energy wave: the sound mode

BN, Gornyi, Titov (2021)

dimensionless linearized equations

$$\tilde{\boldsymbol{q}}\delta\tilde{n}_E - \frac{9\zeta(3)}{2}\left(\tilde{\omega}+i\frac{1+\tilde{q}^2\tilde{\ell}_G^2}{\tilde{\tau}_{\rm dis}}\right)\mathbf{v} = 0$$

$$\left(\tilde{\omega} + i\frac{2\pi\tilde{q}^2\sigma_0}{e^2N\ln 2}\right)\delta\tilde{n} = \frac{2\pi\sigma_0}{eN}\tilde{\boldsymbol{q}}\cdot\boldsymbol{\mathcal{E}}$$

$$\left(\tilde{\omega}+\frac{i}{\tilde{\tau}_R}+\frac{i2\pi\tilde{q}^2\sigma_I}{e^2N\ln 2}\right)\delta\tilde{n}_I - \frac{\pi^2}{6}\tilde{\boldsymbol{q}}\cdot\mathbf{v} - \frac{i4\pi^3\tilde{q}^2\sigma_I\delta\tilde{n}_E}{27\zeta(3)Ne^2\ln 2} = 0$$

$$2\left(\tilde{\omega}+\frac{i}{\tilde{\tau}_{RE}}\right)\delta\tilde{n}_E - \frac{9\zeta(3)}{2}\tilde{\boldsymbol{q}}\cdot\mathbf{v} = 0$$

cosmic sound

separate the energy density

$$\tilde{q}^2\delta\tilde{n}_E = 2\left(\tilde{\omega}+i\frac{1+\tilde{q}^2\tilde{\ell}_G^2}{\tilde{\tau}_{\rm dis}}\right)\left(\tilde{\omega}+\frac{i}{\tilde{\tau}_{RE}}\right)\delta\tilde{n}_E$$

sound mode

$$\tilde{\omega} = \sqrt{\frac{\tilde{q}^2}{2} - \frac{1}{4}\left[\frac{1+\tilde{q}^2\tilde{\ell}_G^2}{\tilde{\tau}_{\rm dis}} - \frac{1}{\tilde{\tau}_{RE}}\right]^2} - i\frac{1+\tilde{q}^2\tilde{\ell}_G^2}{2\tilde{\tau}_{\rm dis}} - \frac{i}{2\tilde{\tau}_{RE}}$$

cosmic sound

$$\omega = v_g q/\sqrt{2}$$

Phan, Song, Levitov (2013)

sound mode dispersion in neutral graphene

BN, Gornyi, Titov (2021)

“full” dispersion

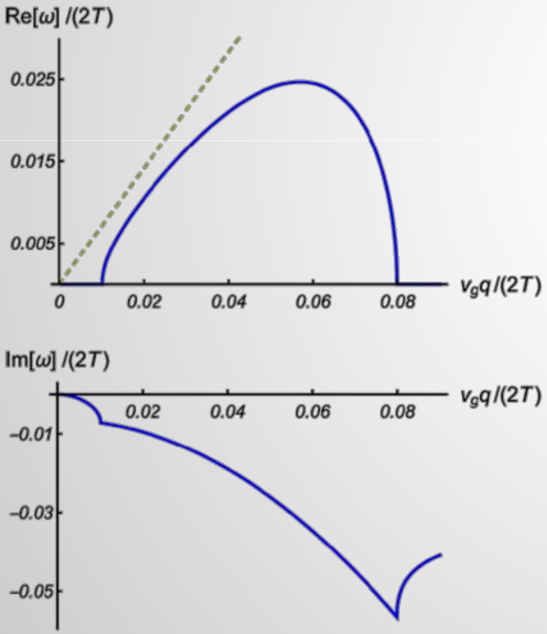

neglecting viscosity and energy relaxation

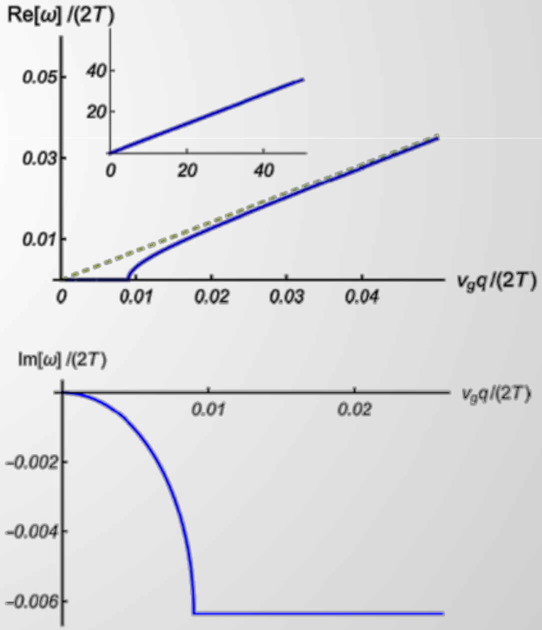

applicability range

BN, Gornyi, Titov (2021)

applicability of hydrodynamic equations

$$q\ell_{\rm hydro} \ll 1, \quad \ell_{\rm hydro} \sim \frac{v_g}{\alpha_g^2 T}$$

sound dispersion should be expanded

$$\frac{v_g^2 q^2}{2} - \frac{\left(1+q^2\ell_G^2\right)^2}{4\tau_{\rm dis}^2} \to \frac{v_g^2 q^2}{2}\left[1 - Aq^2\ell_{\rm hydro}^2 - \mathcal{O}(\tau_{\rm dis}^{-1})\right]$$

simplified dispersion

$$\omega = \sqrt{\frac{v_g^2 q^2}{2} - \frac{1}{4\tau_{\rm dis}^2}} - \frac{i}{2\tau_{\rm dis}}$$

applicability of linear response theory

$$q\ell_{\rm coll} \ll 1, \quad \ell_{\rm coll} \sim \frac{v_g}{\alpha_g^2 T |\ln \alpha_g|} \ll \ell_{\rm hydro}$$

cosmic sound

$$(v_g \tau_{\rm dis})^{-1} \ll q \ll \ell_G^{-1}$$

viscous correction

$$\omega = \frac{v_g q}{\sqrt{2}}\left(1 - \frac{\nu^2 q^2}{4 v_g^2}\right) - \frac{i\nu q^2}{2}$$

cf. Svintsov (2018)

collective modes in doped graphene

BN, Gornyi, Titov (2021)

sound mode in the degenerate regime

gated structure

$$\omega = \sqrt{\frac{v_g^2 q^2}{2}\left[1+\frac{\varkappa}{2\pi C}\right] - \frac{\left(1+\ell_G^2 q^2\right)^2}{4\tau_{\rm dis}^2}} - \frac{i\left(1+\ell_G^2 q^2\right)^2}{2\tau_{\rm dis}}$$

Coulomb interaction

$$\omega = \sqrt{\frac{v_g^2 q^2}{2}\left[1+\frac{\varkappa}{q}\right] - \frac{\left(1+\ell_G^2 q^2\right)^2}{4\tau_{\rm dis}^2}} - \frac{i\left(1+\ell_G^2 q^2\right)^2}{2\tau_{\rm dis}}$$

naïve expansion – is that a plasmon?

$$\omega(q \ll \varkappa) = -\frac{i}{2\tau_{\rm dis}} + \sqrt{\frac{1}{2}v_g^2 q \varkappa - \frac{1}{4\tau_{\rm dis}^2}}$$

zero mode

energy diffusion

$$\omega = -\frac{i}{\tau_{RE}}\frac{\varkappa v_g^2 q^2}{(\varkappa+2\pi C)v_g^2 q^2 + 4\pi C \tau_{RE}^{-1}\tau_{\rm dis}^{-1}}$$

Vlasov self-consistency couples charge and energy

sound mode dispersion obtained neglecting energy relaxation

not a true plasmon – eigenvector is a mix of charge, energy, and velocity fluctuations

sound mode dispersion in doped graphene

BN, Gornyi, Titov (2021)

“weakly doped”

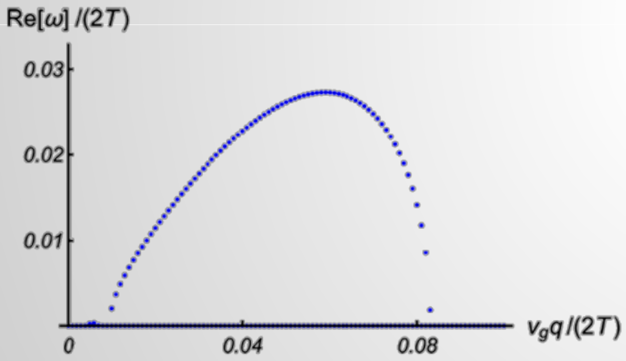

strongly doped, neglecting viscosity and disorder

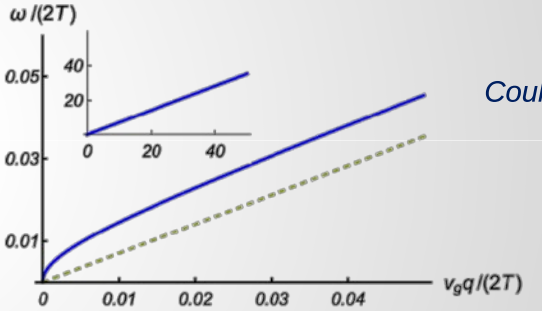

Coulomb interaction

gated structure

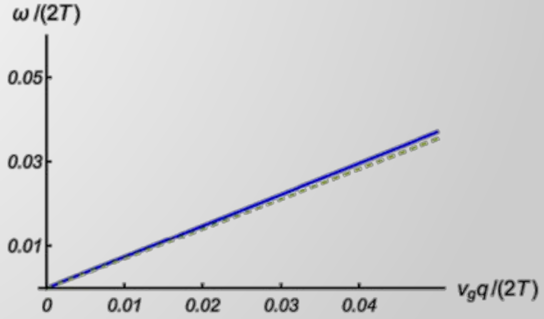

sound mode dispersion in doped graphene

BN, Gornyi, Titov (2021)

strongly doped, with viscosity and disorder

Coulomb interaction

gated structure

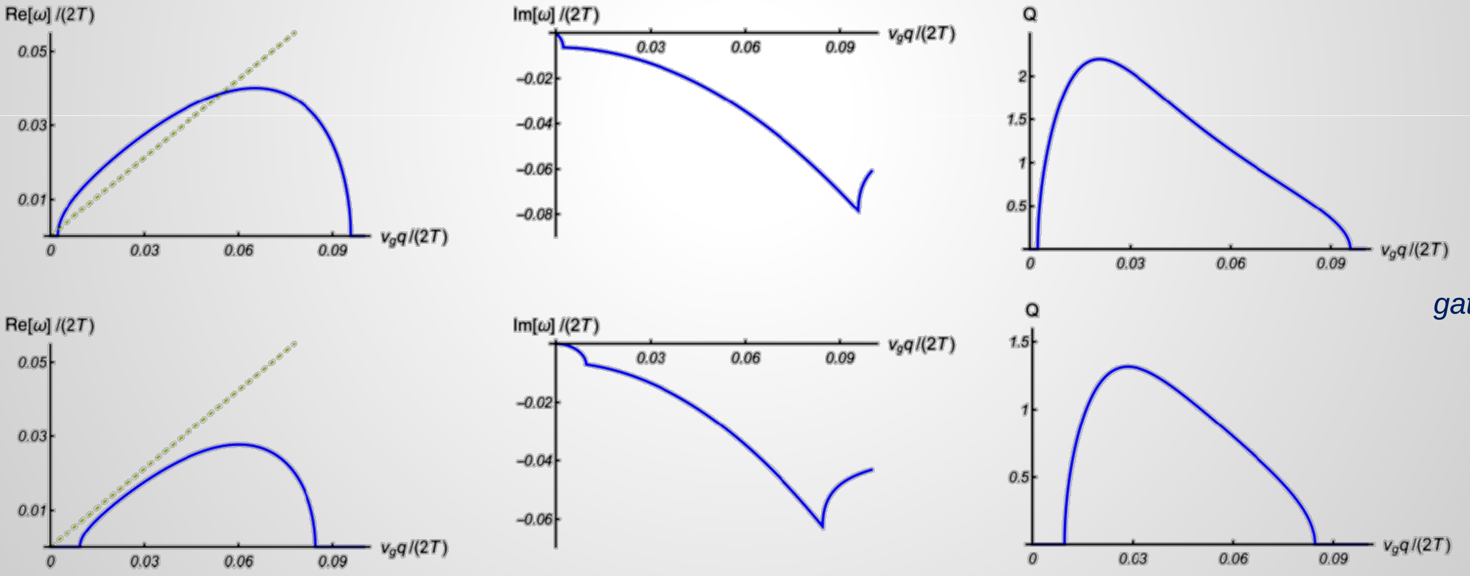

plasmons in doped graphene

plasmons are nonequilibrium collective excitations at higher momenta and frequencies $q\ell_{\rm hydro} > 1$

conventional 2D plasmon

dispersion

Giuliani, Vignale (2005)

$$\omega = \sqrt{2e^2\mu q}\left(1 + \gamma\frac{q}{\varkappa}\right)$$

RPA Lindhard function

$$\gamma = \frac{3}{4}$$

hydrodynamic-like derivation fails yielding a different value

$$\gamma = 1/2$$

neglecting viscosity yields correct dispersion in the presence of disorder

degenerate regime

linear response theory

$$\frac{\partial \boldsymbol{J}}{\partial t} + \frac{v_g^2}{2}\boldsymbol{\nabla}\rho - \nu\Delta\boldsymbol{J} - \frac{v_g^2}{2}\frac{\partial n}{\partial \mu}e^2\boldsymbol{E} = -\frac{\boldsymbol{J}}{\tau_{\rm dis}}$$

beyond the hydrodynamic regime

$$\ell_{\rm hydro}^{-1} \ll q \ll \ell_{\rm coll}^{-1}$$

dispersion for Coulomb interaction

$$\omega = \sqrt{2e^2\mu q\left(1+\frac{q}{\varkappa}\right) - \frac{(1+q^2\ell_G^2)^2}{4\tau_{\rm dis}^2}} - \frac{i(1+q^2\ell_G^2)}{2\tau_{\rm dis}}$$

plasmons in neutral graphene

plasmons are nonequilibrium collective excitations at higher momenta and frequencies $q\ell_{\mathrm{hydro}} > 1$

linear response theory

electric current equation together with the continuity equation yields the plasmon mode

$$\frac{\partial \boldsymbol{j}}{\partial t} + \frac{v_g^2}{2}\boldsymbol{\nabla} n - \frac{2\ln 2}{\pi} e^2 T \boldsymbol{E} = -\frac{\boldsymbol{j}}{\tau_{\mathrm{dis}}} - \frac{\boldsymbol{j}}{\tau_{11}}$$

$$\frac{\partial \boldsymbol{j}_I}{\partial t} + \frac{v_g^2}{2}\boldsymbol{\nabla} n_I - \frac{\gamma_1 \nu}{T}\Delta \boldsymbol{j}_E = -\frac{\boldsymbol{j}_I}{\tau_{\mathrm{dis}}} - \frac{\boldsymbol{j}_I - \frac{\pi^2 \boldsymbol{j}_E}{27\zeta(3)T}}{\tau_{22}\delta_I}$$

$$\frac{\partial \boldsymbol{j}_E}{\partial t} + \frac{v_g^2}{2}\boldsymbol{\nabla} n_E - \nu\Delta \boldsymbol{j}_E = -\frac{\boldsymbol{j}_E}{\tau_{\mathrm{dis}}}$$

energy current equation together with the continuity equation for energy density yields the sound mode

collective modes

plasmon

$$\omega = \sqrt{\frac{v_g^2 \varkappa q}{2}\left(1+\frac{q}{\varkappa}\right) - \frac{v_g^4\varkappa^2}{64\pi^2\sigma_0^2}} - i\frac{v_g^2\varkappa}{8\pi\sigma_0}$$

sound

$$\omega = \sqrt{\frac{v_g^2 q^2}{2} - \frac{\left(1+q^2\ell_G^2\right)^2}{4\tau_{\mathrm{dis}}^2}} - i\frac{1+q^2\ell_G^2}{2\tau_{\mathrm{dis}}}$$

plasmon vs sound in neutral graphene

BN, Gornyi, Titov (2021)

without disorder

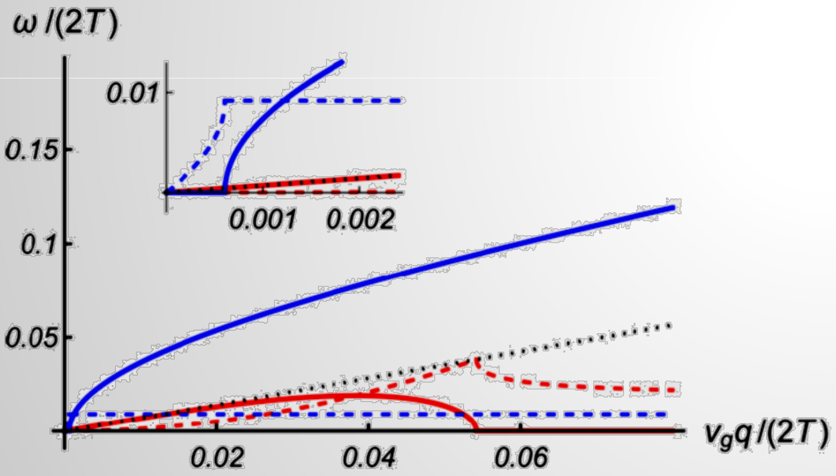

with disorder

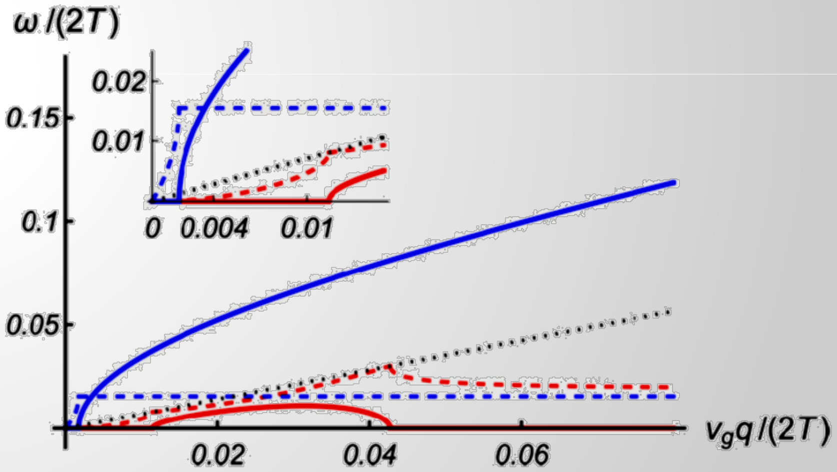

Wiedemann-Franz law violation

Wiedemann-Franz law violation

neglecting viscosity and supercollisions and the related quasiparticle recombination; for review see Lucas, Fong (2018)

linear response currents

neglect viscosity and supercollisions

$$\tau_R \to 0 \quad \Rightarrow \quad \mu_I = 0; \qquad \eta \to 0$$

linear response

$$\boldsymbol{J} = e\left[\frac{v_g^2 \tau_{\rm dis} \bar{n}^2}{3\bar{P}} + \bar{\Sigma}_{11}\right]\left[e\boldsymbol{E} - T\boldsymbol{\nabla}\frac{\mu}{T}\right] - \frac{e v_g^2 \tau_{\rm dis} \bar{n}}{T}\boldsymbol{\nabla}T$$

$$\boldsymbol{Q} = \left[v_g^2 \tau_{\rm dis} \bar{n}\left(1 - \frac{\bar{\mu}\bar{n}}{3\bar{P}}\right)\right]\left[e\boldsymbol{E} - T\boldsymbol{\nabla}\frac{\mu}{T}\right]$$

$$- \frac{v_g^2 \tau_{\rm dis}}{T}\left(3\bar{P} + \bar{\mu}\bar{n}\right)\boldsymbol{\nabla}T$$

kinetic coefficients

$$\sigma = e^2 \frac{v_g^2 \tau_{\rm dis} \bar{n}^2}{3\bar{P}} + e^2 \bar{\Sigma}_{11} \qquad \kappa = \frac{3\bar{P}}{\bar{T}} v_g^2 \tau_{\rm dis} \frac{e^2 \bar{\Sigma}_{11}}{\sigma}$$

Lorentz number at charge neutrality

conductivity

$$\sigma(\mu = 0) = e^2 \bar{\Sigma}_{11} = \frac{2\ln 2}{\pi} e^2 \bar{T} \frac{\tau_{11}\tau_{\rm dis}}{\tau_{11} + \tau_{\rm dis}} \to \mathcal{A}\frac{e^2}{\alpha_g^2}$$

thermal conductivity

$$\kappa(\mu = 0) \to \frac{3\bar{P}}{\bar{T}} v_g^2 \tau_{\rm dis} = \frac{18\zeta(3)}{\pi} \bar{T}^2 \tau_{\rm dis}$$

Lorentz number

$$L(\mu = 0) = \frac{27\zeta(3)}{\pi^2 \ln 2}\left(1 + \frac{\tau_{\rm dis}}{\tau_{11}}\right) L_0 = \mathcal{C}_0 L_0$$

$$\mathcal{C}_0(\alpha_g = 0.23,\ \tau_{\rm dis}^{-1} = 0.8\,\mathrm{THz},\ T = 298\,\mathrm{K}) = 53.4$$

Wiedemann-Franz law violation

neglecting viscosity and supercollisions and the related quasiparticle recombination; for review see Lucas, Fong (2018)

linear response currents

neglect viscosity and supercollisions

$$\tau_R \to 0 \quad \Rightarrow \quad \mu_I = 0; \qquad \eta \to 0$$

linear response

$$\boldsymbol{J} = e\left[\frac{v_g^2 \tau_{\text{dis}} \bar{n}^2}{3\bar{P}} + \bar{\Sigma}_{11}\right]\left[e\boldsymbol{E} - T\boldsymbol{\nabla}\frac{\mu}{T}\right] - \frac{e v_g^2 \tau_{\text{dis}} \bar{n}}{T}\boldsymbol{\nabla}T$$

$$\boldsymbol{Q} = \left[v_g^2 \tau_{\text{dis}} \bar{n}\left(1 - \frac{\bar{\mu}\bar{n}}{3\bar{P}}\right)\right]\left[e\boldsymbol{E} - T\boldsymbol{\nabla}\frac{\mu}{T}\right]$$

$$- \frac{v_g^2 \tau_{\text{dis}}}{T}\left(3\bar{P} + \bar{\mu}\bar{n}\right)\boldsymbol{\nabla}T$$

kinetic coefficients

$$\sigma = e^2 \frac{v_g^2 \tau_{\text{dis}} \bar{n}^2}{3\bar{P}} + e^2 \bar{\Sigma}_{11} \qquad \kappa = \frac{3\bar{P}}{T} v_g^2 \tau_{\text{dis}} \frac{e^2 \bar{\Sigma}_{11}}{\sigma}$$

Lorentz number in the degenerate regime

conductivity

$$\sigma(x = \mu/T \gg 1) \to \frac{e^2}{\pi}\bar{\mu}\tau_{\text{dis}}\left(1 + \frac{\pi^4}{3x^2(\pi^2 + x^2\tau_{\text{dis}}/\tau_{11})}\right)$$

thermal conductivity

$$\bar{T}\kappa(x \gg 1) = \frac{1}{\pi}\bar{\mu}^3\tau_{\text{dis}} \frac{\frac{\pi^4}{3x^2(\pi^2 + x^2\tau_{\text{dis}}/\tau_{11})}}{1 + \frac{\pi^4}{3x^2(\pi^2 + x^2\tau_{\text{dis}}/\tau_{11})}}$$

Lorentz number

$$L(x \gg 1) = \frac{\pi^2}{3e^2}\frac{1}{1 + \frac{x^2\tau_{\text{dis}}}{\pi^2\tau_{11}}} = \mathcal{C}_{FL} L_0$$

$$\mathcal{C}_{FL} \approx \frac{1}{1 + \frac{4\alpha_g^2}{3\pi}\bar{\mu}\tau_{\text{dis}}} \ll 1$$

anti-Poiseuille flow in neutral graphene

viscosity in graphene near charge neutrality

Schütt, BN (2019)

hydrodynamics at charge neutrality

electric current

$$\boldsymbol{j} = n\boldsymbol{u} + \delta\boldsymbol{j} = \delta\boldsymbol{j}$$

generalized Stokes (linear) equation

$$\boldsymbol{\nabla} P = \eta\Delta\boldsymbol{u} + \frac{e}{c}\delta\boldsymbol{j}\times\boldsymbol{B} - \frac{3P\boldsymbol{u}}{v_g^2\tau_{\rm dis}}$$

in the absence of magnetic field, the electric current in neutral graphene is not hydrodynamic

BN, Gornyi, Titov (2021)

understanding of boundary conditions is key to interpret experimental data: channel geometry does not support Poiseuille flow!

viscosity at arbitrary densities

Harvard group (2020)

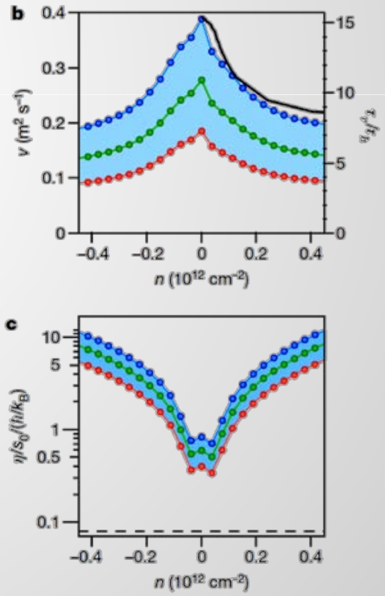

diffusive to ballistic crossover

in confined geometries, electron motion is governed by the ratio of the mean free path to the sample size

boundary conditions for distribution function

Beenakker, van Houten (1991)

slab geometry

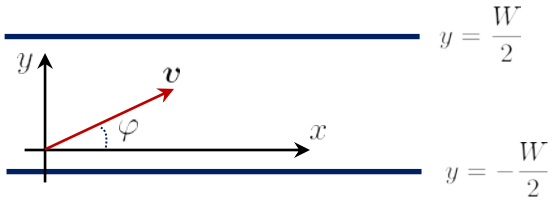

diffusive scattering at the boundary

$$f = f_0 + \delta f(y, \varphi)$$

$$\delta f\left(\frac{W}{2}; -\pi < \varphi < 0\right) = \frac{1}{2}\int_0^{\pi} d\varphi' \cos\varphi' \delta f\left(\frac{W}{2}; \varphi'\right)$$

outgoing *incoming*

current profile in the slab geometry

$$J_x \propto 4\int_0^1 dz\sqrt{1-z^2}\left[1 - e^{-\frac{1}{\ell z}}\cosh\frac{y}{\ell z}\right]$$

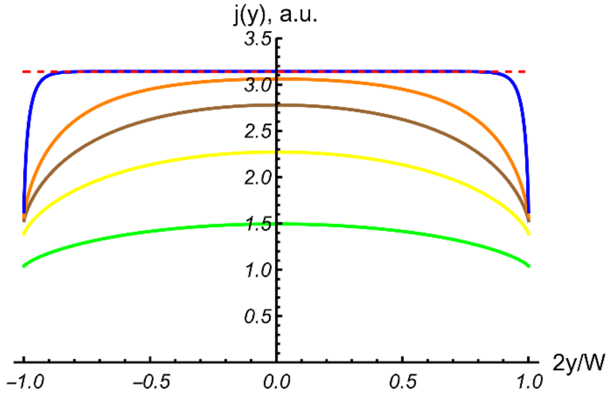

anti-Poiseuille flow in neutral graphene

in neutral graphene subjected to magnetic field the electronic flow is inhomogeneous

absence of Poiseuille flow in zero field

BN, Gornyi, Titov (2021)

absence of longitudinal hydrodynamic flow

$$\eta \frac{\partial^2 u_x}{\partial y^2} = \frac{3 P u_x}{v_g^2 \tau_{\rm dis}} \quad \Rightarrow \quad u_x = 0$$

Coulomb drag-like resistivity

$$\boldsymbol{J} = \frac{1}{R_0} \boldsymbol{E}, \qquad R_0 = \frac{\pi}{2 \ln 2} \frac{1}{e^2 T} \left(\frac{1}{\tau_{11}} + \frac{1}{\tau_{\rm dis}} \right)$$

Poiseuille-like flow of energy can be induced by applying a temperature gradient

Link, BN, Kiselev, Schmalian (2018)

anti-Poiseuille flow

BN, Gornyi, Titov (2021)

magnetic field couples the longitudinal current and lateral neutral quasiparticle (energy) flows leading to inhomogeneity

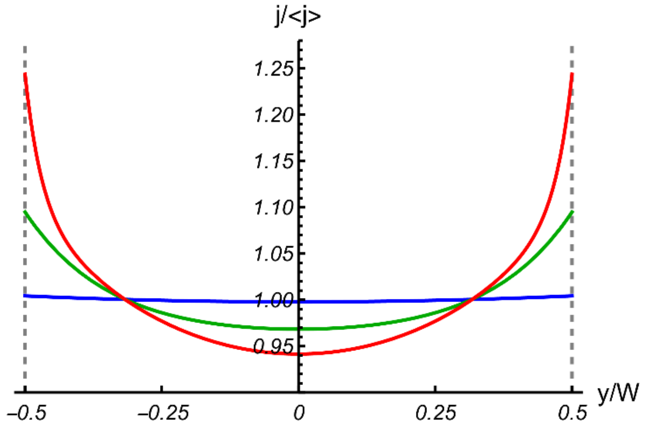

two-band phenomenology at charge neutrality

electron hydrodynamics in neutral graphene

Alekseev et.al, (2015)

edge vs bulk

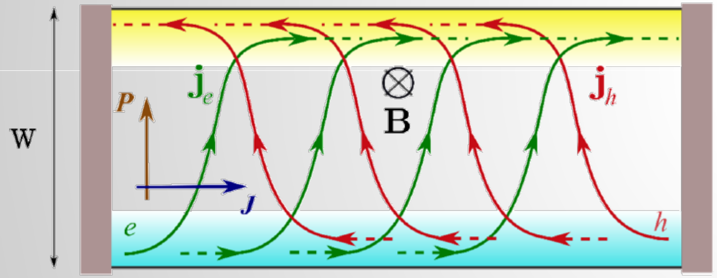

key to understand nonlocal transport experiments in graphene

linear magnetoresistance

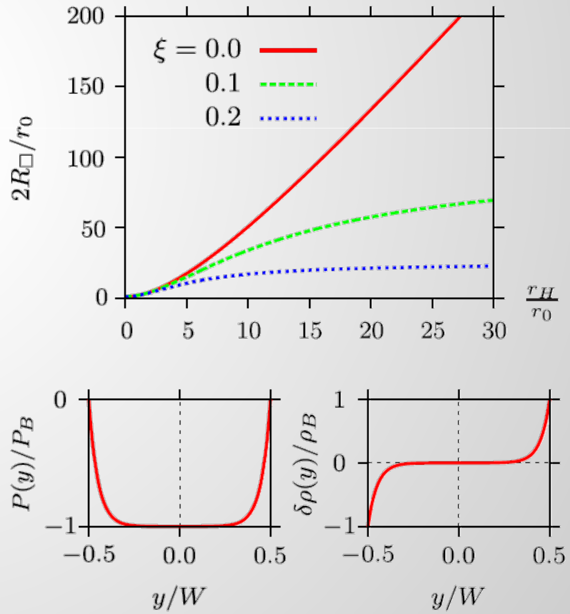

numerical solution of phenomenological equations

Danz, Titov, BN (2020)

two-band phenomenology

macroscopic currents (“Ohm’s Law”)

$$\boldsymbol{j} + eD(\nu_e + \nu_h)\boldsymbol{E} + \omega_c\tau\boldsymbol{j}_I \times \boldsymbol{e}_B + D\boldsymbol{\nabla}n = 0$$

$$\boldsymbol{j}_I + eD(\nu_e - \nu_h)\boldsymbol{E} + \omega_c\tau\boldsymbol{j} \times \boldsymbol{e}_B + D\boldsymbol{\nabla}\rho = 0$$

continuity equations

$$\boldsymbol{\nabla}\cdot\boldsymbol{j} = 0 \qquad \boldsymbol{\nabla}\cdot\boldsymbol{j}_I = -\frac{\delta\rho}{\tau_R}$$

Vlasov selfconsistency (gated structure)

$$\boldsymbol{E} = \boldsymbol{E}_0 - \frac{e}{C}\boldsymbol{\nabla}n$$

degenerate regime (single band)

Ohmic flow in the absence of magnetic field

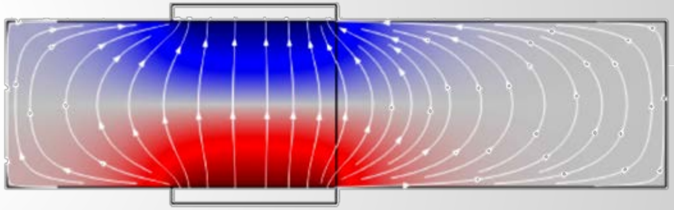

classical Hall effect

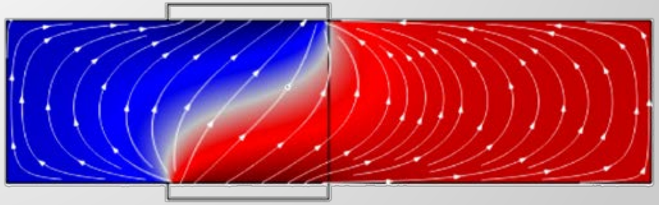

numerical solution of phenomenological equations

Danz, Titov, BN (2020)

two-band phenomenology

macroscopic currents (“Ohm’s Law”)

$$\boldsymbol{j} + eD(\nu_e + \nu_h)\boldsymbol{E} + \omega_c\tau\boldsymbol{j}_I \times \boldsymbol{e}_B + D\boldsymbol{\nabla}n = 0$$

$$\boldsymbol{j}_I + eD(\nu_e - \nu_h)\boldsymbol{E} + \omega_c\tau\boldsymbol{j} \times \boldsymbol{e}_B + D\boldsymbol{\nabla}\rho = 0$$

continuity equations

$$\boldsymbol{\nabla}\cdot\boldsymbol{j} = 0 \qquad \boldsymbol{\nabla}\cdot\boldsymbol{j}_I = -\frac{\delta\rho}{\tau_R}$$

Vlasov selfconsistency (gated structure)

$$\boldsymbol{E} = \boldsymbol{E}_0 - \frac{e}{C}\boldsymbol{\nabla}n$$

charge neutrality (two bands)

Ohmic flow in the absence of magnetic field

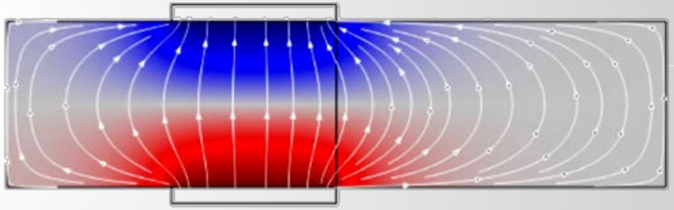

nonlocality in magnetic field

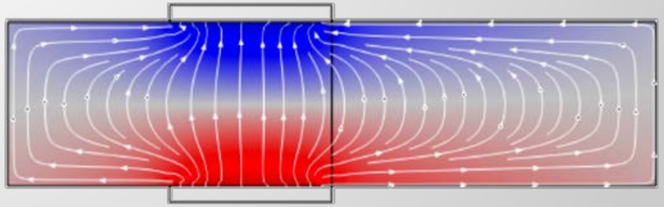

numerical solution of phenomenological equations

Danz, Titov, BN (2020)

nonlocal response: current density

Ohmic flow in the absence of magnetic field

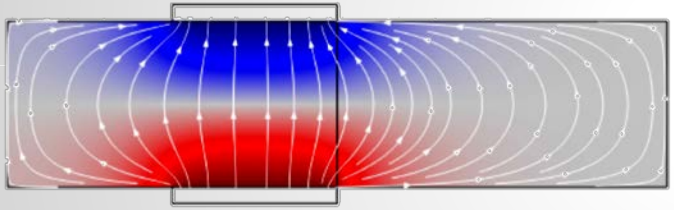

nonlocality on magnetic field

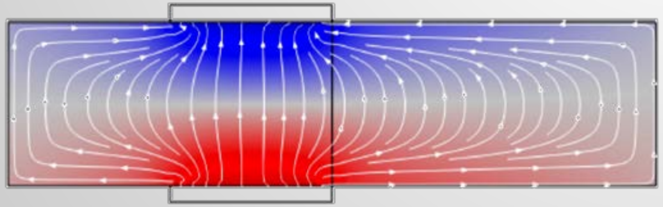

nonlocal resistance

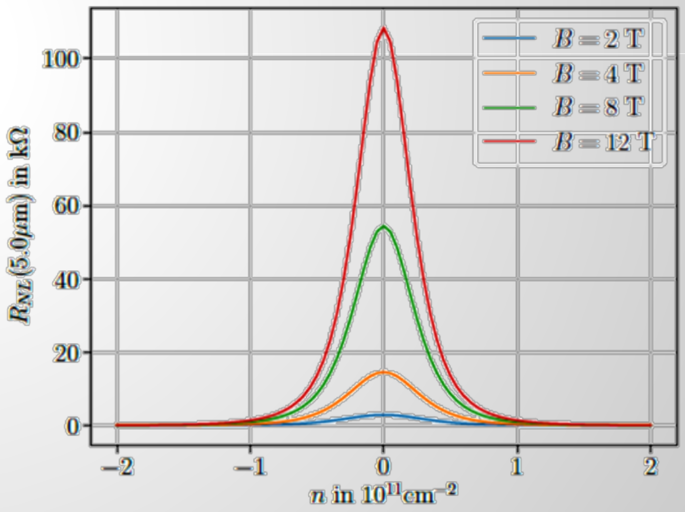

Corbino geometry

neutral graphene: Corbino geometry

in Corbino disks the electronic flow is always inhomogeneous; there are no boundaries limiting lateral flow, hence no compensated Hall effect; boundaries with contacts are important and feature additional contact resistance due to viscous dissipation in the bulk

electric field "expulsion" in doped graphene

Shavit, Shytov, Falkovich (2019)

Gurzhi equation

$$e\boldsymbol{E} = -m\nu\Delta\boldsymbol{u} + \frac{m\boldsymbol{u}}{\tau_{\rm dis}}$$

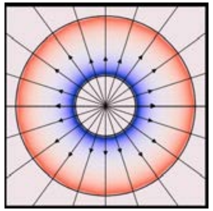

continuity equation

$$\boldsymbol{\nabla}\boldsymbol{u} = 0 \quad \rightarrow \quad u_r \propto \frac{1}{r}$$

viscous term vanishes for Ohmic flow

$$\Delta[u_r(r)\boldsymbol{e}_r] = \left[\frac{\partial}{\partial r}\frac{1}{r}\frac{\partial}{\partial r}(ru_r)\right]\boldsymbol{e}_r \quad \rightarrow 0$$

paradox: viscosity does not affect current flow;
in the clean limit the electric field vanishes

no expulsion in neutral graphene

Gall, BN, Gornyi (2023)

electric current

$$\boldsymbol{j} = n\boldsymbol{u} + \delta\boldsymbol{j} = \delta\boldsymbol{j} \qquad \delta\boldsymbol{j} = \frac{\boldsymbol{E}}{eR_0}$$

hydrodynamic velocity

$$\eta'\Delta\boldsymbol{u} = \frac{3P\boldsymbol{u}}{v_g^2\tau_{\rm dis}} \qquad \eta' = \eta + \frac{3P\tau_{RE}}{2}$$

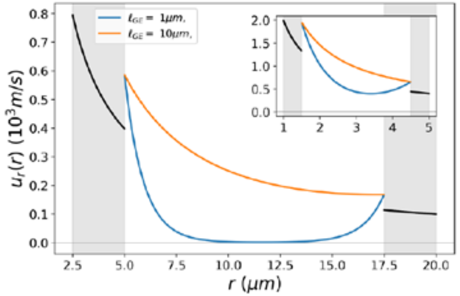

neutral graphene: Corbino geometry

in Corbino disks the electronic flow is always inhomogeneous; there are no boundaries limiting lateral flow, hence no compensated Hall effect; boundaries with contacts are important and feature additional contact resistance due to viscous dissipation in the bulk

viscous dissipation in doped graphene

Shavit, Shytov, Falkovich (2019)

energy dissipation rate due to viscosity

$$\mathcal{A} = \frac{1}{2\eta}\int \sum_{i,j} (\sigma_{ij})^2 dV > 0$$

work by the current source $\mathcal{A} = \phi_0 I$

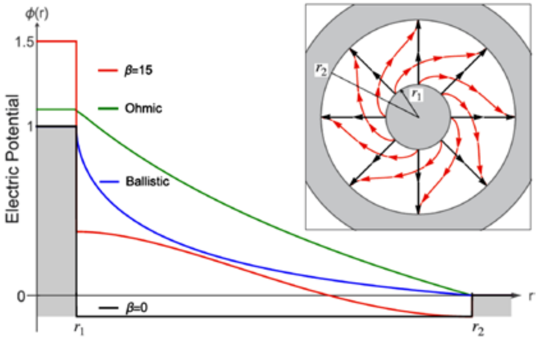

viscous dissipation in neutral graphene

Gall, BN, Gornyi (2023)

dissipation rate

$$\mathcal{A} = \dot{\mathcal{E}} = \int dS_\beta \left(u_\alpha \sigma'_{\alpha\beta} - u_\beta \delta P - e\delta j_\beta \phi \right)$$

potential jump

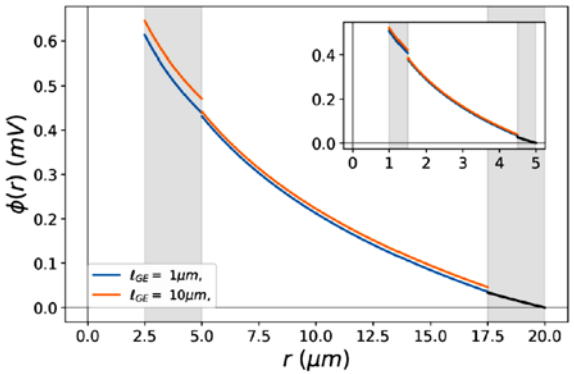

neutral graphene: Corbino geometry in magnetic field

Gall, BN, Gornyi (2023)

velocity vs current

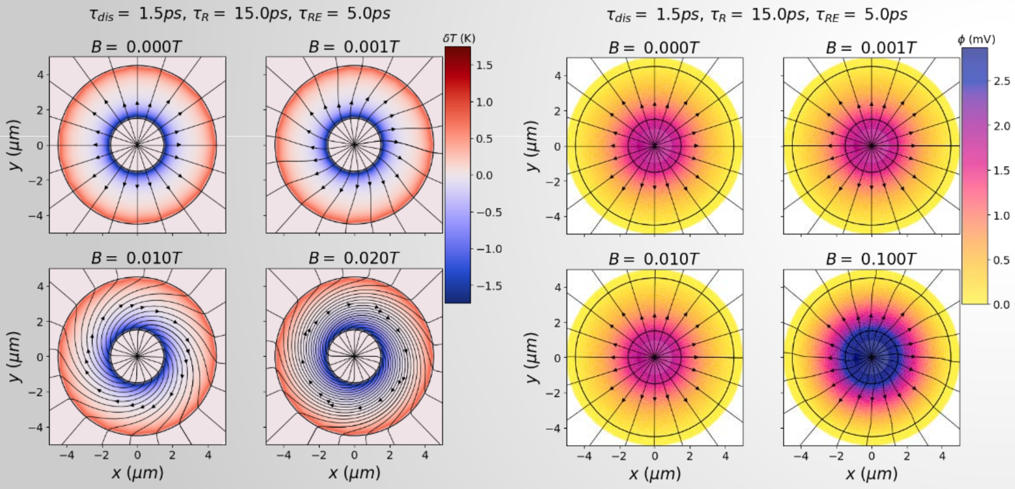

a possible method for measuring electronic viscosity at charge neutrality

parabolic magnetoresistance

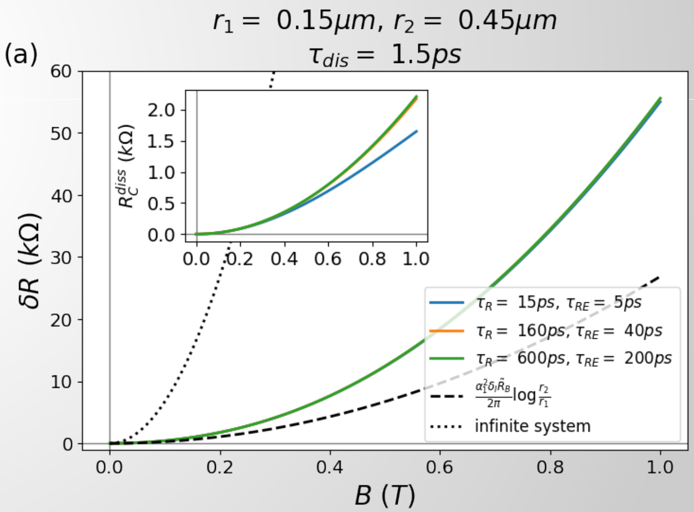

optical conductivity

optical conductivity in neutral graphene

Wang group (2019)

Quantum-critical scattering rates

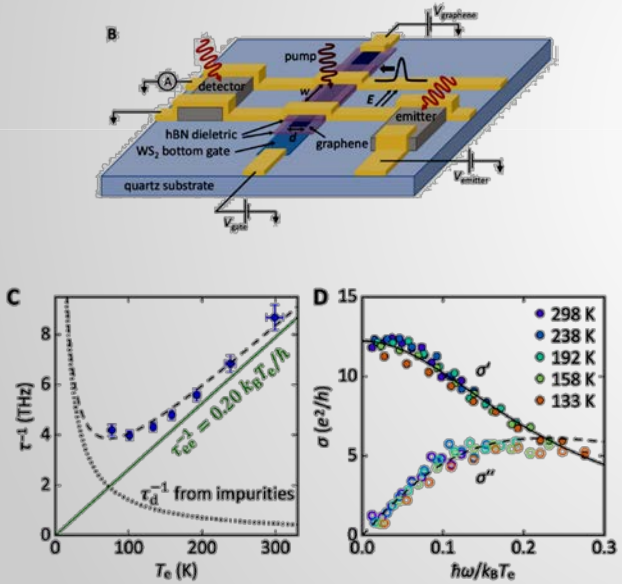

optical conductivity in hydrodynamics

hydrodynamic contribution

$$\sigma_h = \frac{e^2 v_g^2 n^2}{W} \frac{1}{\tau_{\text{dis}}^{-1} - i\omega}$$

kinetic contribution

$$\sigma_k(\mu = 0) = \frac{2\ln 2}{\pi} \frac{e^2 T}{\tau_{\text{dis}}^{-1} + \tau_{11}^{-1} - i\omega}$$

Sun, Basov, Fogler (2018); BN (2019)

$$\tau_{11}^{-1} \propto \alpha_g^2 T$$

Kashuba (2008); Fritz et.al (2008)

optical conductivity

in systems exhibiting collective behavior, optical conductivity can still be approximated by a Lorentzian

bad metals

Delacretaz, Gouteraux, Hartnoll, Karlsson (2015)

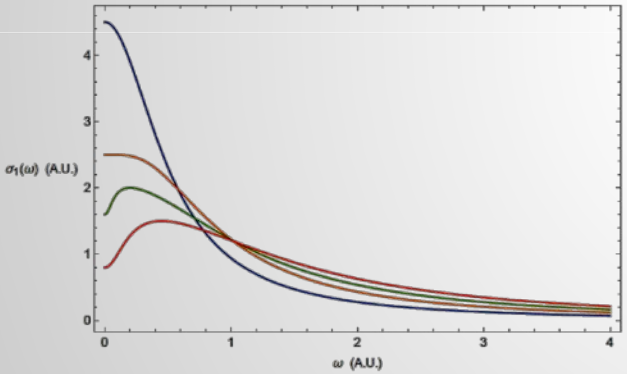

Figure 1: Illustrative plot of the temperature dependence of the optical conductivity of bad metals. As temperature is increased, the peak broadens and then moves off the $\omega = 0$ axis.

graphene in hydrodynamic regime

BN (2019)

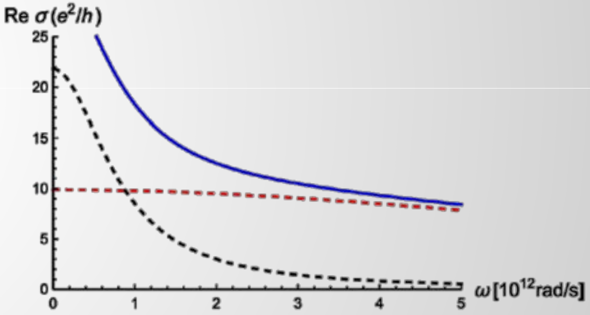

FIG. 2. Optical conductivity in weakly doped graphene at $n = 0.08\,\mathrm{cm}^{-12}$ [or $E_F = 33\,\mathrm{meV}$, the value used in Ref. [1]; see Fig. 4(b) of that reference]. The almost flat red dashed curve shows the real part of the kinetic contribution (15b), while the black dashed curve shows the real part of the hydrodynamic contribution (21). The real part of the full electrical conductivity (i.e., the sum $\delta\sigma + \sigma_h$) is shown by the solid blue curve. The curves were calculated with $\alpha_g = 0.23$, $T = 298\,\mathrm{K}$, and $\tau_{\mathrm{dis}}^{-1} = 0.8\,\mathrm{THz}$, the values taken from Ref. [1].

conjectured hydrodynamics in strongly correlated systems

lower bound on viscosity

most known hydrodynamic systems are characterized by a viscosity to entropy density ratio that is larger than a certain universal value; this statement might not be literally applicable to anisotropic systems

AdS/CFT correspondence

Kovtun, Son, Starinets (2005)

$$\frac{\eta}{s} \geqslant \frac{\hbar}{4\pi k_B}$$

uncertainty principle interpretation

$$\eta \propto \tau n_E, \qquad s \propto k_B n$$

$$\frac{\eta}{s} \propto \frac{\tau n_E}{k_B n} \gtrsim \frac{\hbar}{k_B}$$

anisotropic Dirac systems

Link, BN, Kiselev, Schmalian (2018)

Inkof, Küppers. Link, Gouteraux, Schmalian (2020)

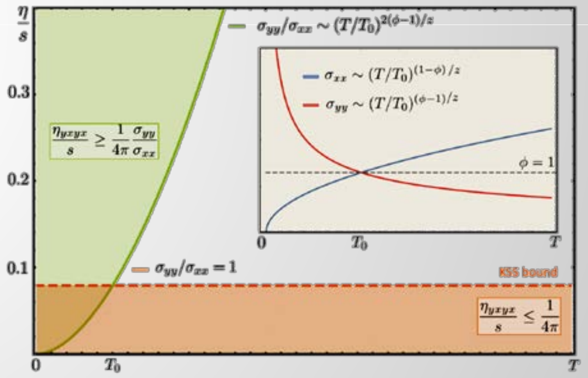

Figure 1. Main panel: temperature dependence of the η/s tensor. In the anisotropic case the KSS bound (orange) can be parametrically violated (green line). Here, T_0 is a temperature scale below which the anisotropy effects are dominant. The conductivity ratio might constitute a new lower bound when rotations are broken (green). Inset: temperature dependence of the conductivity tensor elements σ_{xx} and σ_{yy}. ϕ is the crossover exponent that characterizes the anisotropy between the different spatial directions $k_x \sim k_y^{1/\phi}$. Once $\phi \neq 0$ one element of the conductivity of a two-dimensional system must be insulating and the other must be metallic.

limiting bounds on charge transport

In an incoherent metal, transport is controlled by the collective diffusion of energy and charge rather than by quasiparticle or momentum relaxation.

violation of the Mott-Ioffe-Regel limit

Hartnoll (2015)

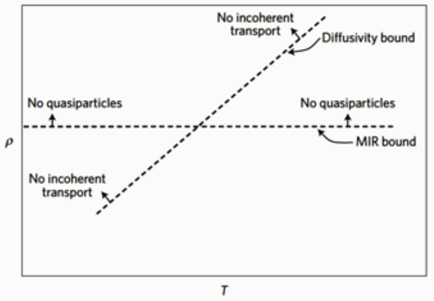

Figure 1 | Quasiparticle bounds versus incoherent bounds. Schematic illustration of the role of the MIR bound and the proposed diffusivity bound in the resistivity versus temperature plane.

$$D_c \geqslant C_D \frac{\hbar v^2}{k_B T}$$

$$\rho \sim \frac{k_B T}{\hbar v_F^2 \chi}$$

"Planckian relaxation"

Mackenzie group (2013)

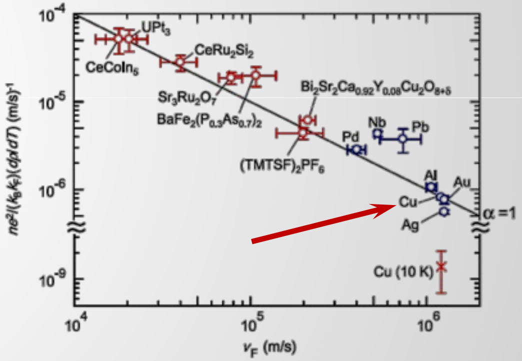

Fig. 2. In spite of two orders of magnitude variations in their Fermi velocities (v_F), a wide range of metals in which the resistivity varies linearly with temperature have similar scattering rates per kelvin. These include heavy fermion, oxide, pnictide, and organic metals for which T-linear resistivity can be seen down to low temperatures with appropriate tuning by magnetic field, chemical composition, or hydrostatic pressure, and more conventional metals for which T-linear resistivity is seen at high temperatures (blue symbols). At low temperatures, the scattering rate per kelvin of a conventional metal is orders of magnitude lower, as illustrated for the case of Cu at 10 K, shown in the lower right hand corner (*11*). On the graph, the line marked $\alpha = 1$ corresponds to $(\tau T)^{-1} = k_B/\hbar$. The near-universality of the scattering rates is observed in spite of the fact that the scattering mechanisms vary across the range of materials. The point for $Bi_2Sr_2Ca_{0.92}Y_{0.08}Cu_2O_{8+\delta}$ is based on the value $\alpha = 1.3$, which is determined from optical conductivity (*21*), combined with the measured value of v_F for this material (*44*). For all others, the analysis is based on resistivity data combined with knowledge of the Fermi volume and average Fermi velocity. Full details of the determination of the parameters in the axis labels are given in (*11*).

optical conductivity

in systems exhibiting collective behavior, optical conductivity can still be approximated by a Lorentzian

bad metals

Delacretaz, Gouteraux, Hartnoll, Karlsson (2015)

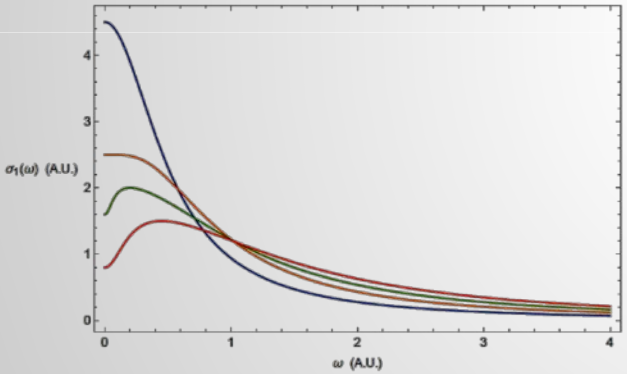

Figure 1: Illustrative plot of the temperature dependence of the optical conductivity of bad metals. As temperature is increased, the peak broadens and then moves off the $\omega = 0$ axis.

graphene in hydrodynamic regime

BN (2019)

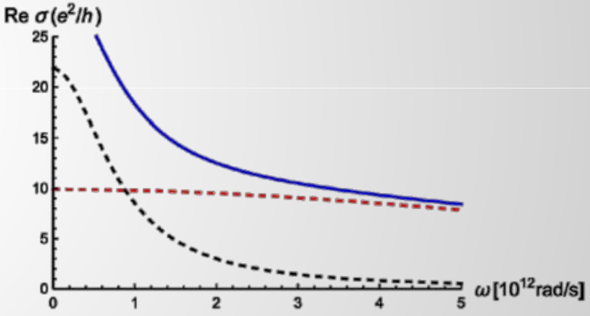

FIG. 2. Optical conductivity in weakly doped graphene at $n = 0.08\,\mathrm{cm}^{-12}$ [or $E_F = 33\,\mathrm{meV}$, the value used in Ref. [1]; see Fig. 4(b) of that reference]. The almost flat red dashed curve shows the real part of the kinetic contribution (15b), while the black dashed curve shows the real part of the hydrodynamic contribution (21). The real part of the full electrical conductivity (i.e., the sum $\delta\sigma + \sigma_h$) is shown by the solid blue curve. The curves were calculated with $\alpha_g = 0.23$, $T = 298\,\mathrm{K}$, and $\tau_{\mathrm{dis}}^{-1} = 0.8\,\mathrm{THz}$, the values taken from Ref. [1].

concluding remarks

electronic hydrodynamics: not boring, not 100% clear

experimental puzzles

nonlocal transport : bulk vs edge

low Lorentz numbers in topological materials

no “smoking gun”?

conjectured generalizations

universal linear resistivity

why should different materials saturate the proposed bounds?

what is the mechanism behind splitting into charge and energy modes?

Coulomb effects in electronic transport – work in progress!

small corrections

quantum corrections to conductivity

fluctuation effects

higher-order effects

entire effects

Coulomb drag

electronic hydrodynamics

Wigner crystal

open problems

strange (bad) metals

strongly-correlated systems

unconventional superconductivity